Theory: ground state properties and the limits of the region of superheavy elements.

Anatoli Afanasjev

Mississippi State University

1. Stabilization mechanism
2. Shell structure, spherical and deformed shell gaps, density profiles
3. Evolution of shapes and fission barriers as a function of Z and A

2. Stabilization mechanisms

Physics of superheavy nuclei

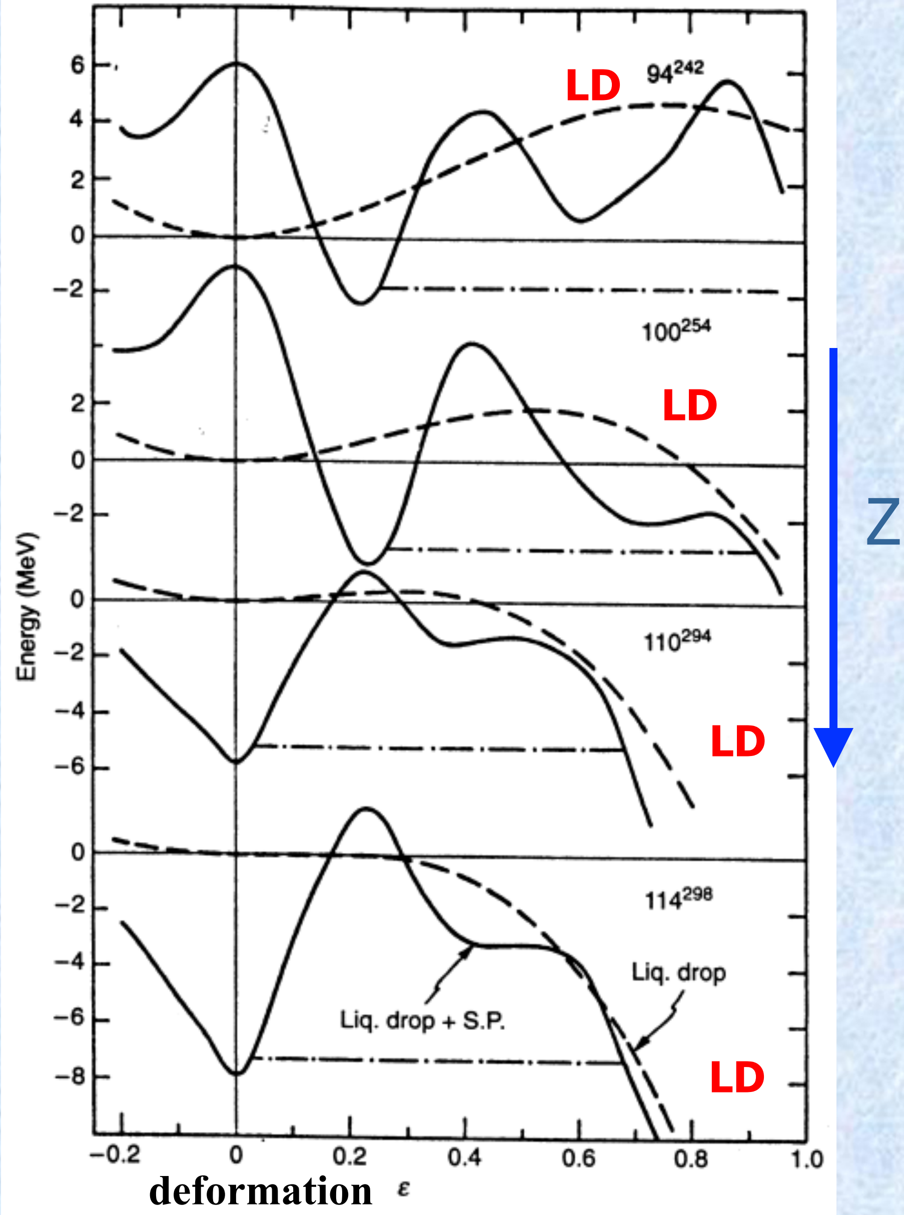

Macroscopic + microscopic approach

$$E_{tot} = E_{LD} + \delta E_{shell} + E_{pair}$$

liquid drop

quantum (shell) correction

pairing

Liquid-drop fission barrier vanishes

Stability of superheavy nuclei is determined exclusively by quantum (shell) effects

1. Shell structure, spherical and deformed shell gaps, density profiles

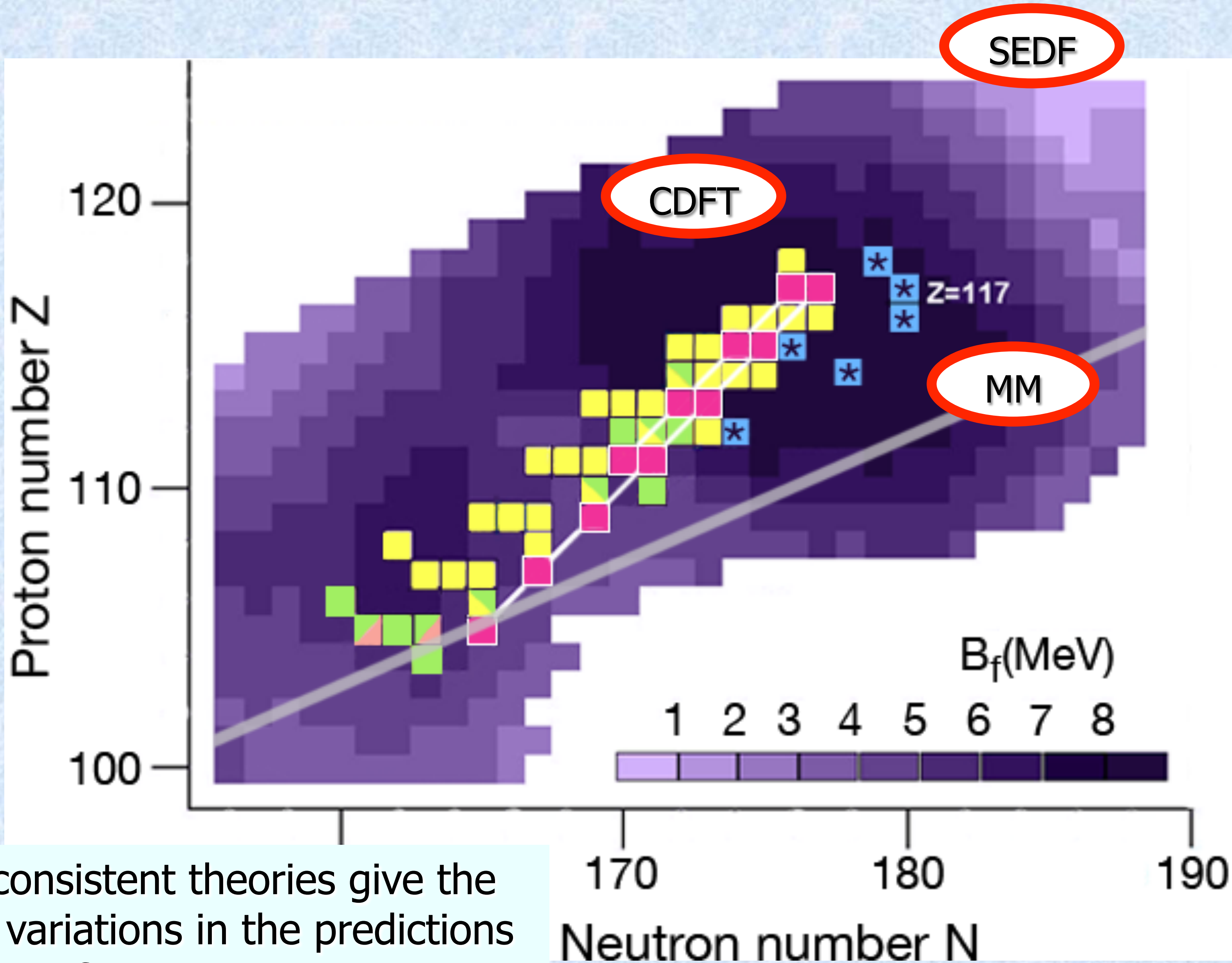

Self-consistent theories give the largest variations in the predictions of magic gaps

at Z=120, 126 and 172, 184

Dependence of proton Z=120 and neutron N=172 gaps on CDFT parametrization

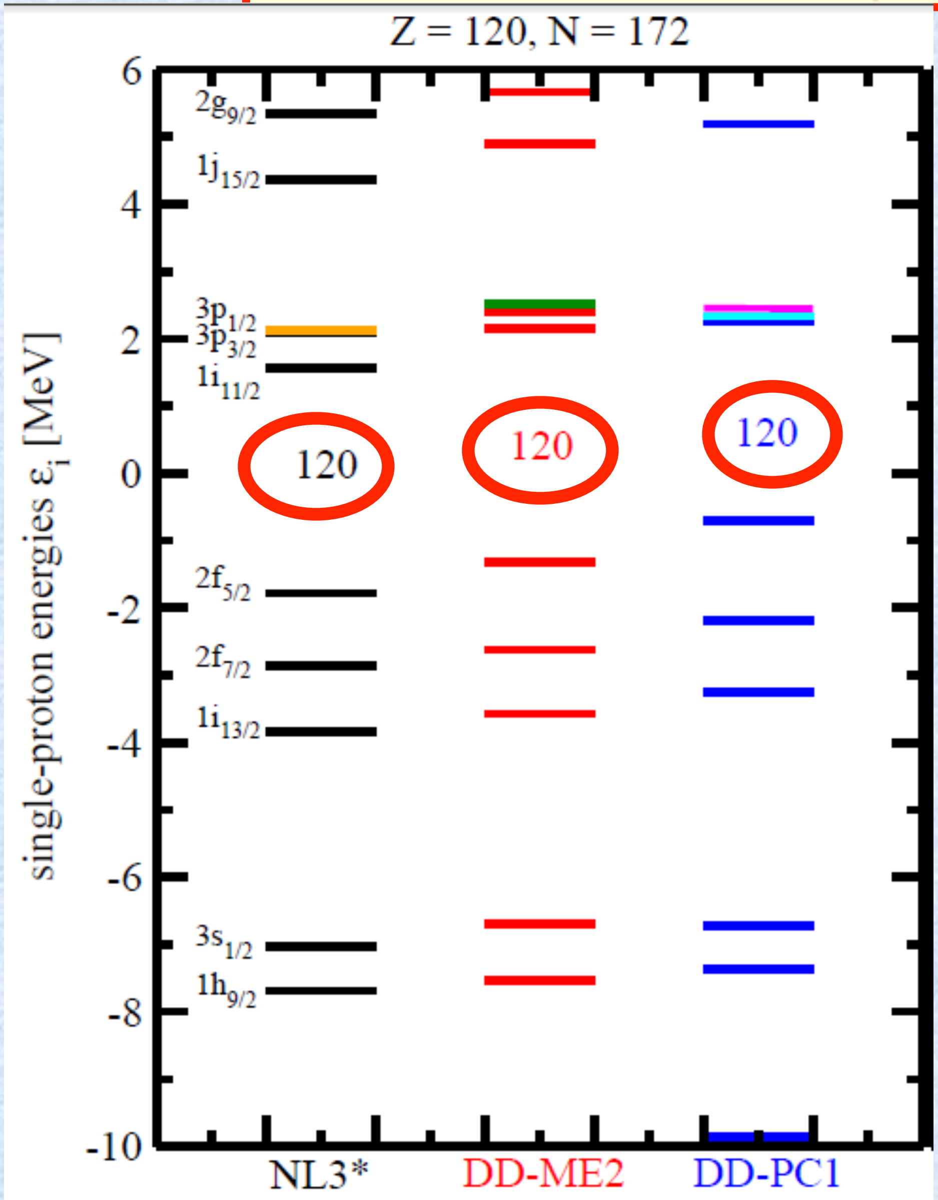

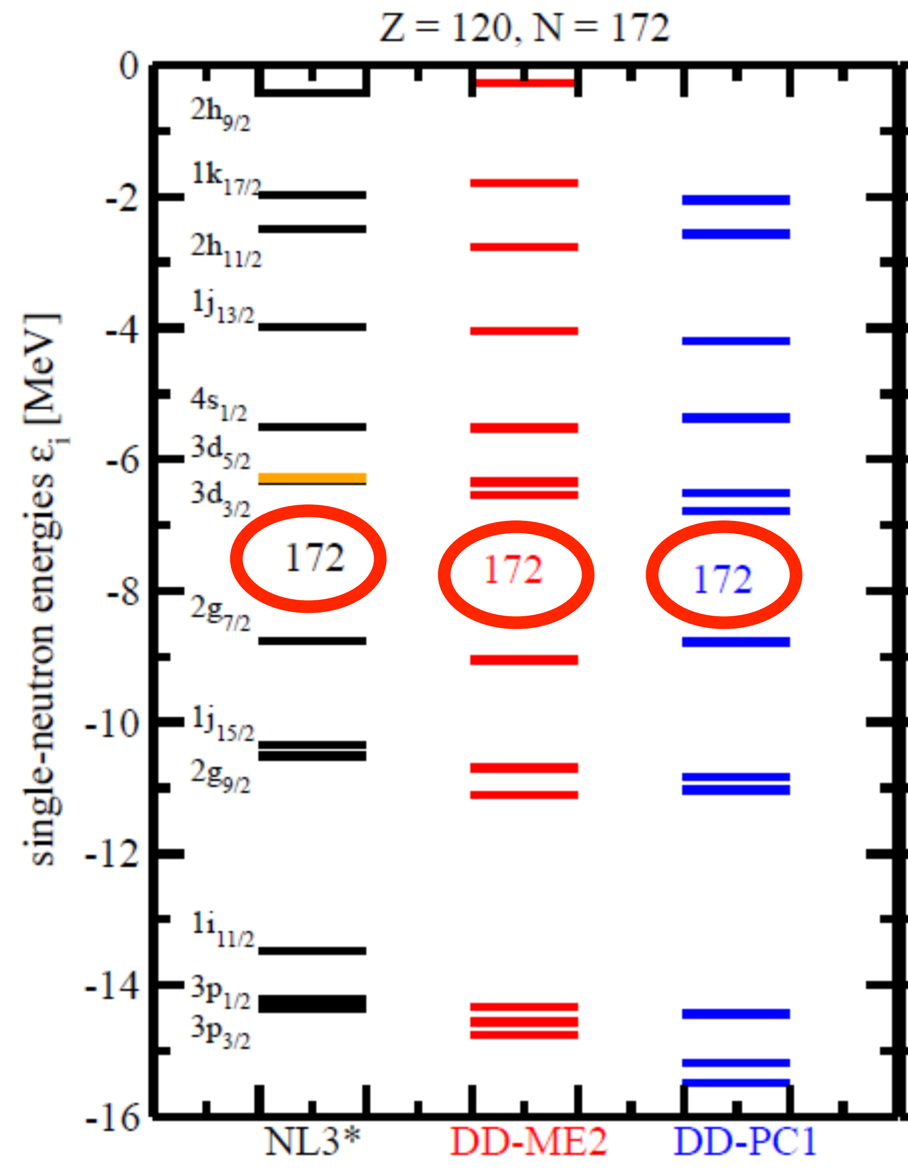

How magic are "magic" shell gaps?

Calculated spherical Z=120 gap versus experimental deformed Z=100 gap

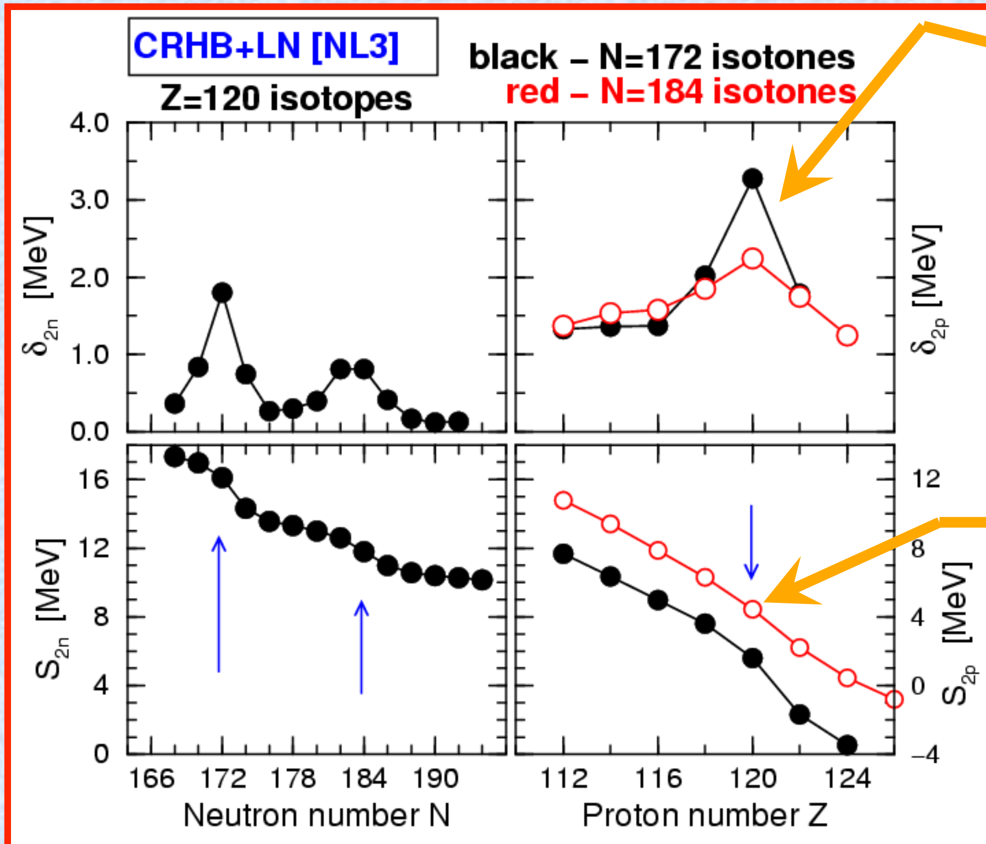

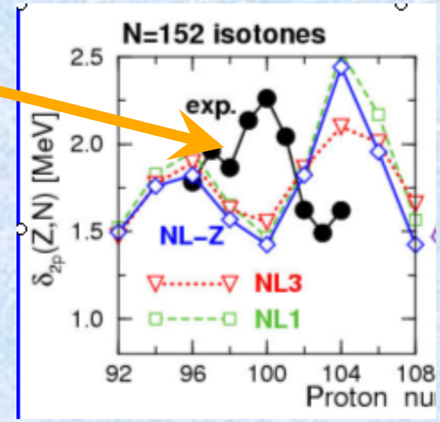

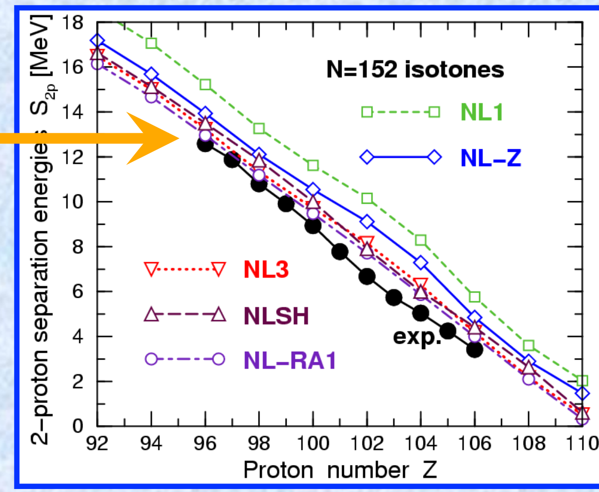

Similar relation for neutron spherical N=172 and deformed N=152 gap

It might be that the effect of spherical shell gaps in superheavy nuclei is only 30-40% more pronounced than the effect of deformed gaps in the A~250 region

Shell correction energy: difference between tin and SHE regions

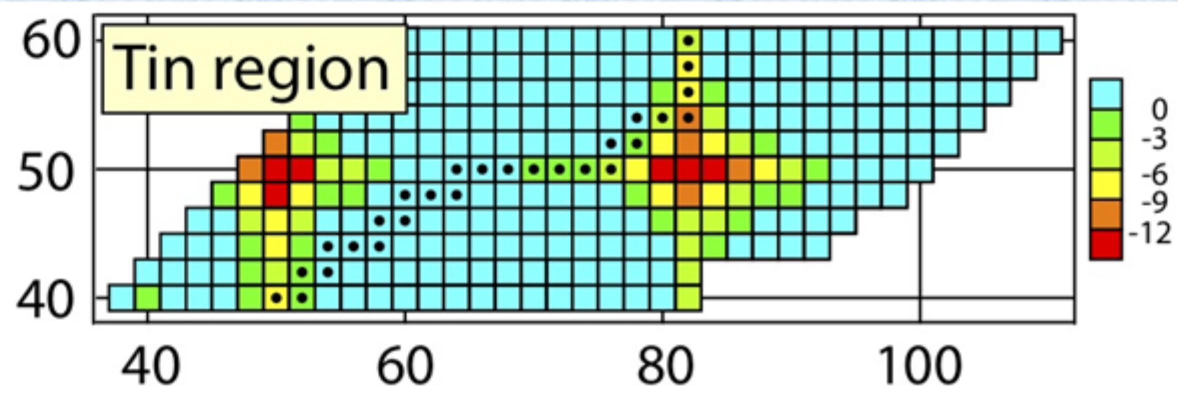

M.Bender, W.Nazarewicz,
P.-G.Reinhard,
PLB 515, 42 (2001)

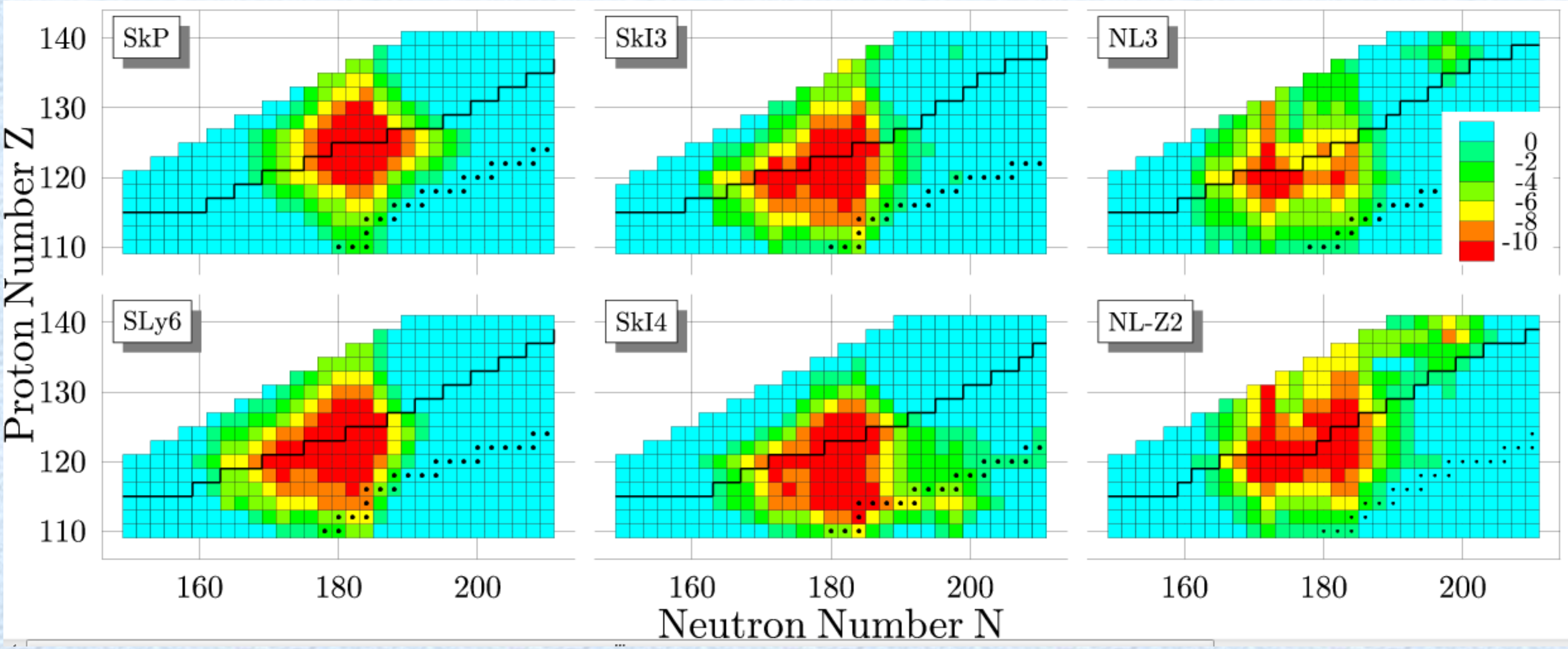

What are the possible sources of different centers of the islands of SHE?

- **self-consistency effects [density profiles]**

may explains mic+mac vs DFT

- **spin-orbit splittings**

may explain CDFT versus Skyrme DFT

Densities of superheavy nuclei: spherical RMF calculations with the NL3 force

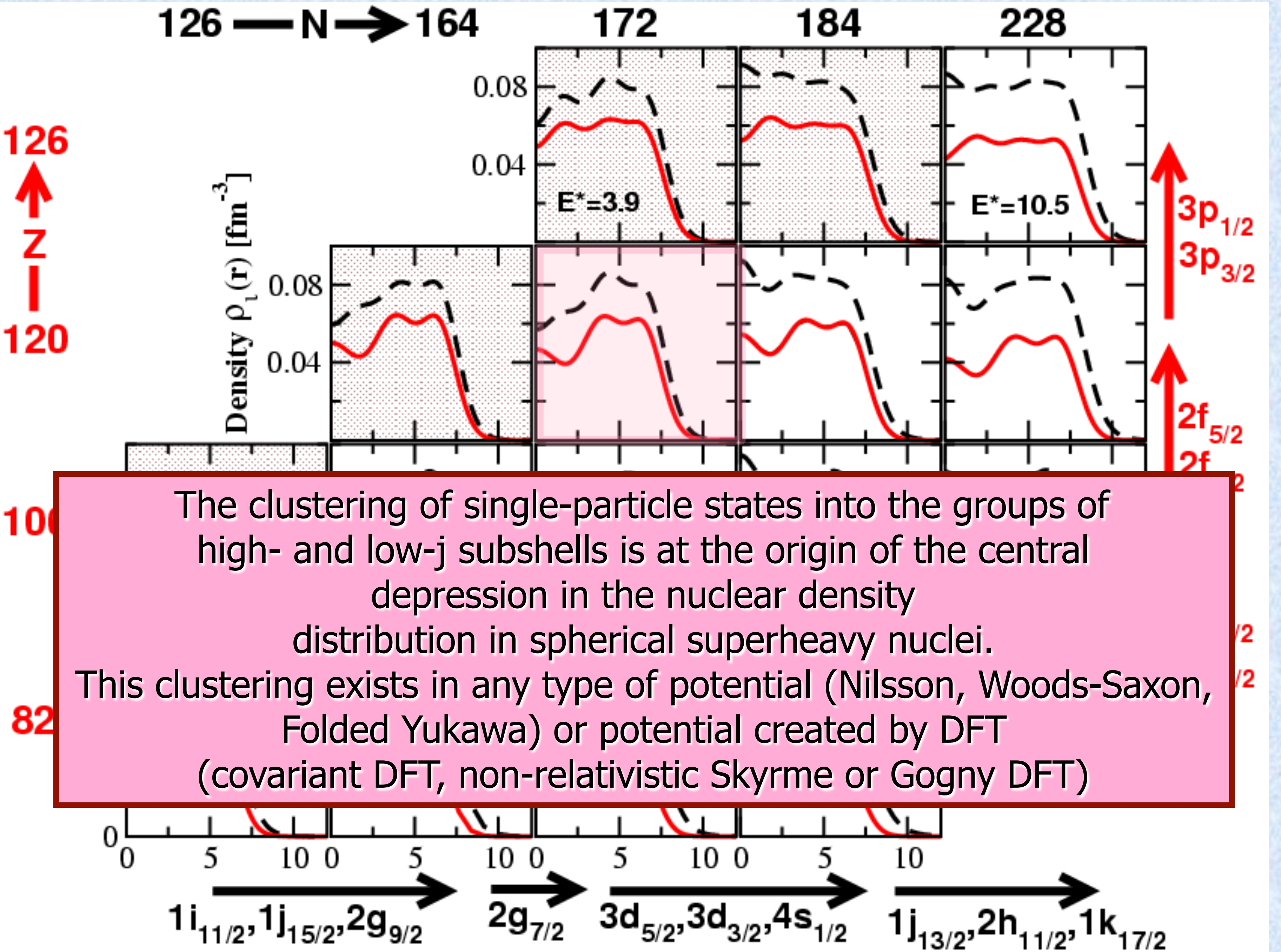

The clustering of single-particle states into the groups of high- and low-j subshells is at the origin of the central depression in the nuclear density distribution in spherical superheavy nuclei.

This clustering exists in any type of potential (Nilsson, Woods-Saxon, Folded Yukawa) or potential created by DFT (covariant DFT, non-relativistic Skyrme or Gogny DFT)

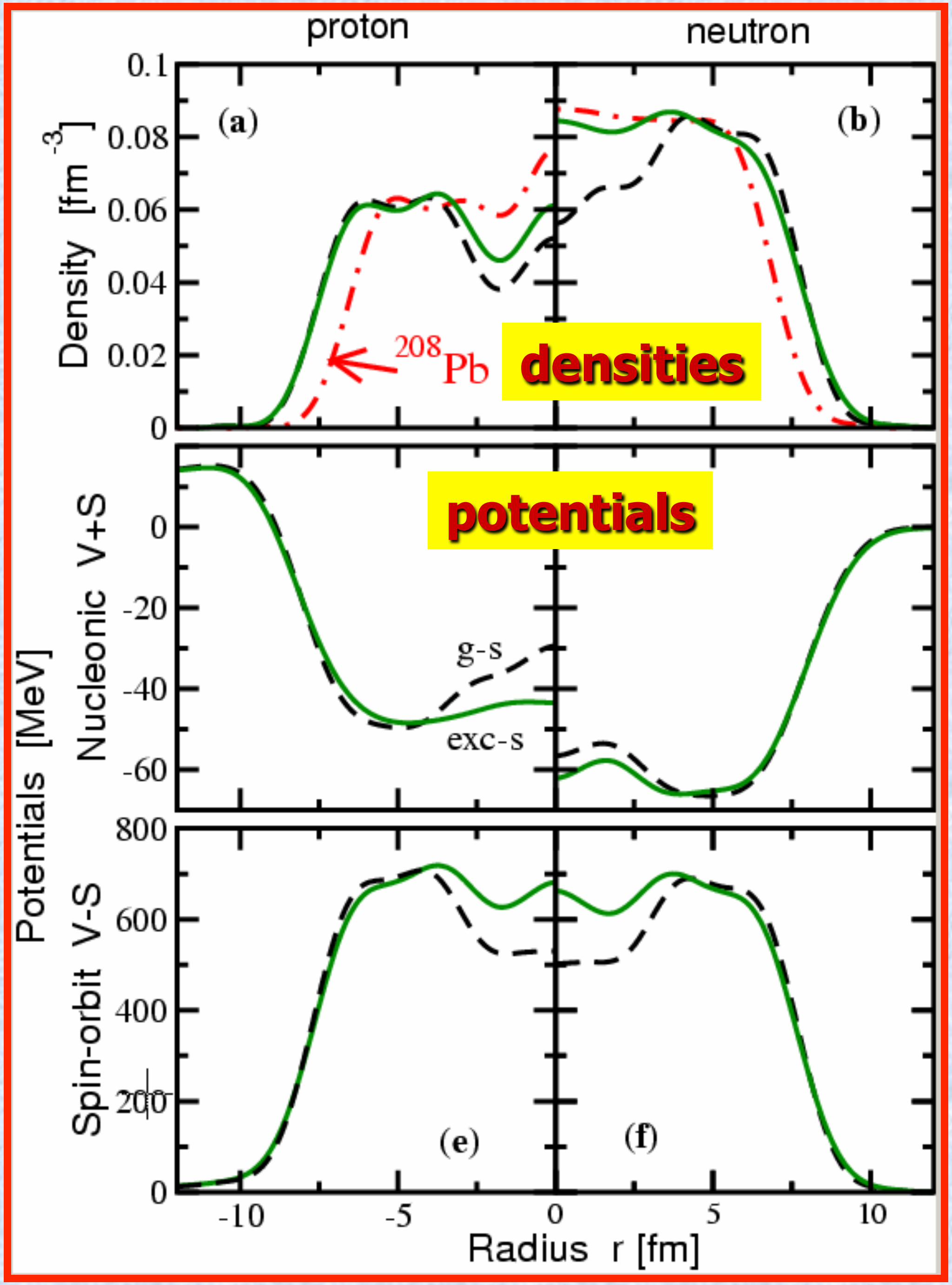

AA and S.Frauendorf, PRC 71, 024308 (2005)

Impact of particle-hole excitations on the densities and potentials (nucleonic, spin-orbit)

General conclusion (tested on large # of particle-hole excitations in different nuclei):

1. **Large density depression** in the central part of nucleus: **shell gaps at Z=120, N=172**

2. **Flat density distribution** in the central part of nucleus: **Z=126 appears, N=184 becomes larger and Z=120 (N=172) shrink**

Skyrme SkP [m*/m=1]
double shell closure at Z=126, N=184
(SkM*, **????**

Skyrme SkI3 [m*/m=0.57]
gaps at Z=120, N=184
no double shell closure,
SLy6

Gogny D1S
Z=120, N=172(?)
Z=126, N=184

RMF
double shell closure at Z=120, N=172

Large effective mass m*/m~0.8-1.0

Low effective mass m*/m ~ 0.65

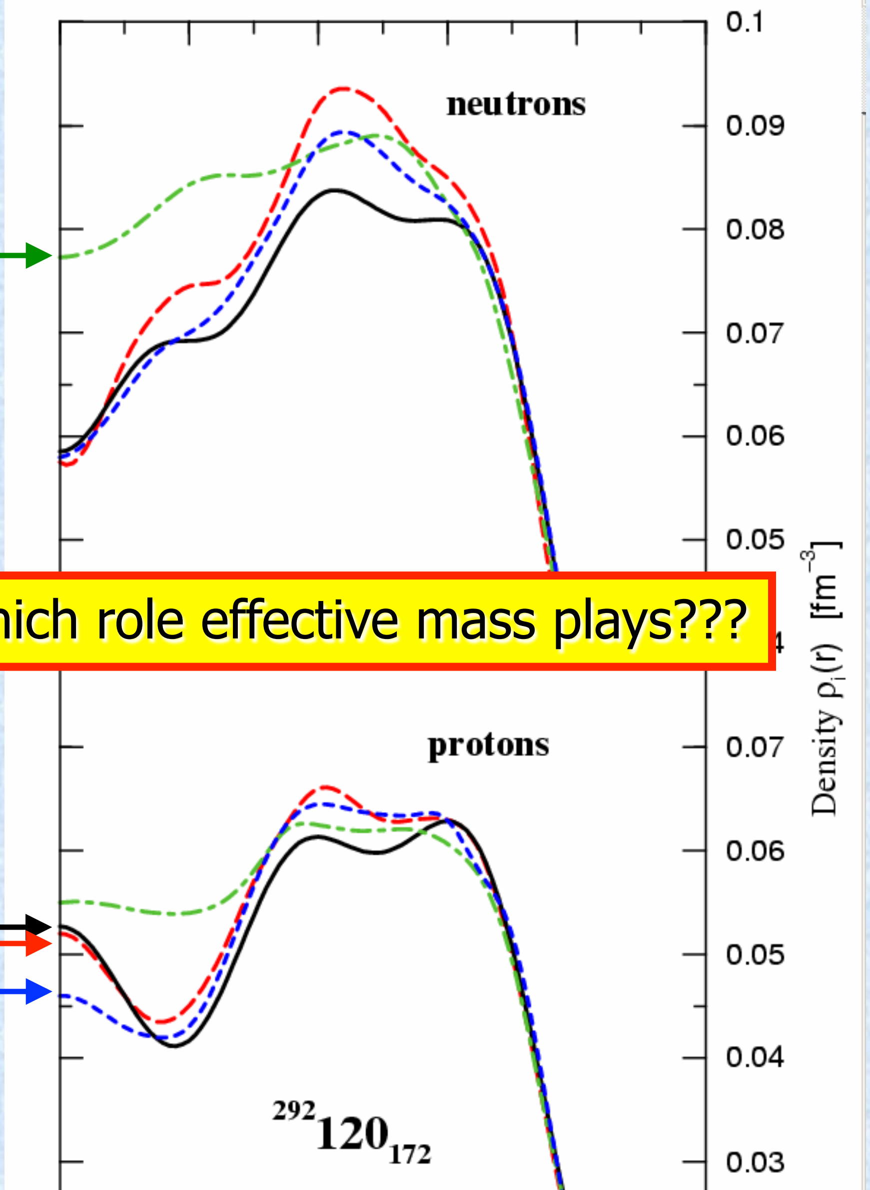

Which role effective mass plays???

RHB: Densities in paired and unpaired calculations are almost the same

Semiclassical result:

1. $m^*/m \sim 1$ at the surface; <1 in the interior

2. Classically, nucleons with given kinetic energy are more likely to be found in regions with high effective mass than in the regions with low one because they travel with lower speed.

3. The increase of the effective mass in the surface region favors the transfer of mass from the center there.

Spin-orbit splitting

Spin – orbit interaction – fully relativistic phenomenon

PVC; E.V. Litvinova and AA, PRC 84, 014305 (2011)

Mean field level;
M.Bender et al, PRC 60 (1999) 034304

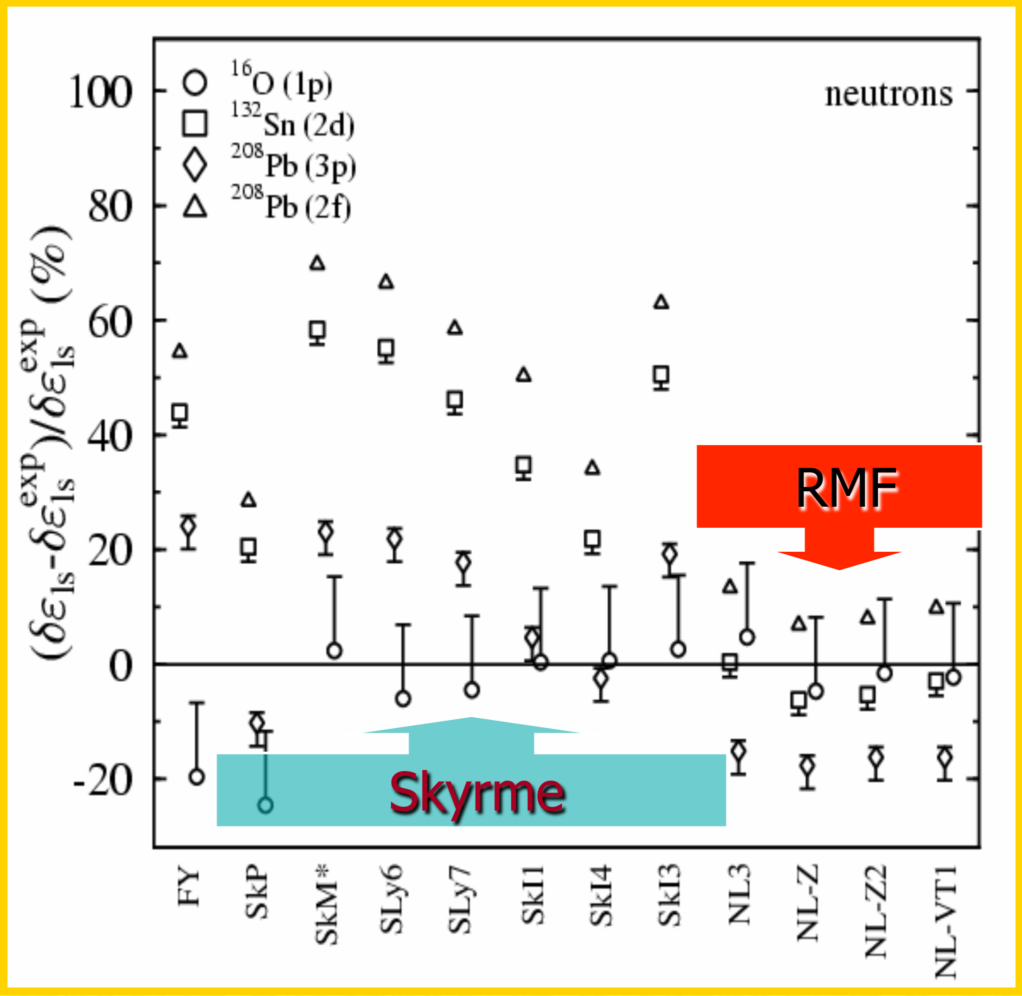

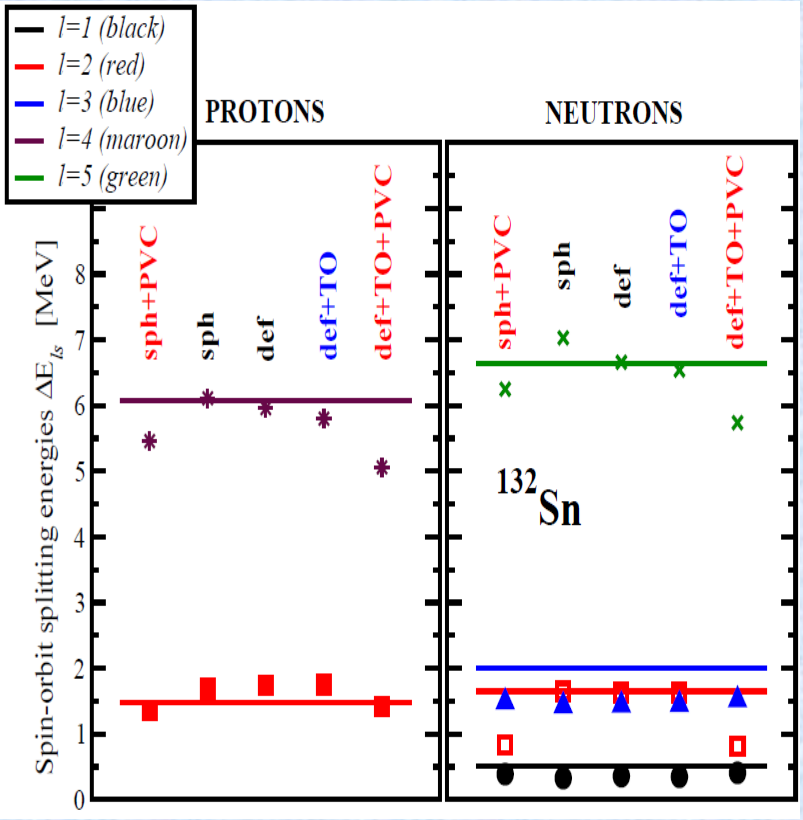

The absolute deviations per doublet are **0.34 MeV** **[0.50 MeV],** **0.23 MeV** **[0.56 MeV]** and **0.26 MeV** **[0.45 MeV]** **in the mean field** ("def+TO") [**particle-vibration coupling** ("def+TO+PVC")] calculations in ^{56}Ni, ^{132}Sn and ^{208}Pb, respectively.

Particle-vibrational corrections to single-particle spectra of superheavy elements.

Even in the presence of particle-vibration coupling the Z=120 shell gap still persist, the N=172 shell gap is smaller and thus somewhat more questionable.

E. Litvinova, AA, PRC 84, 014305 (2011)

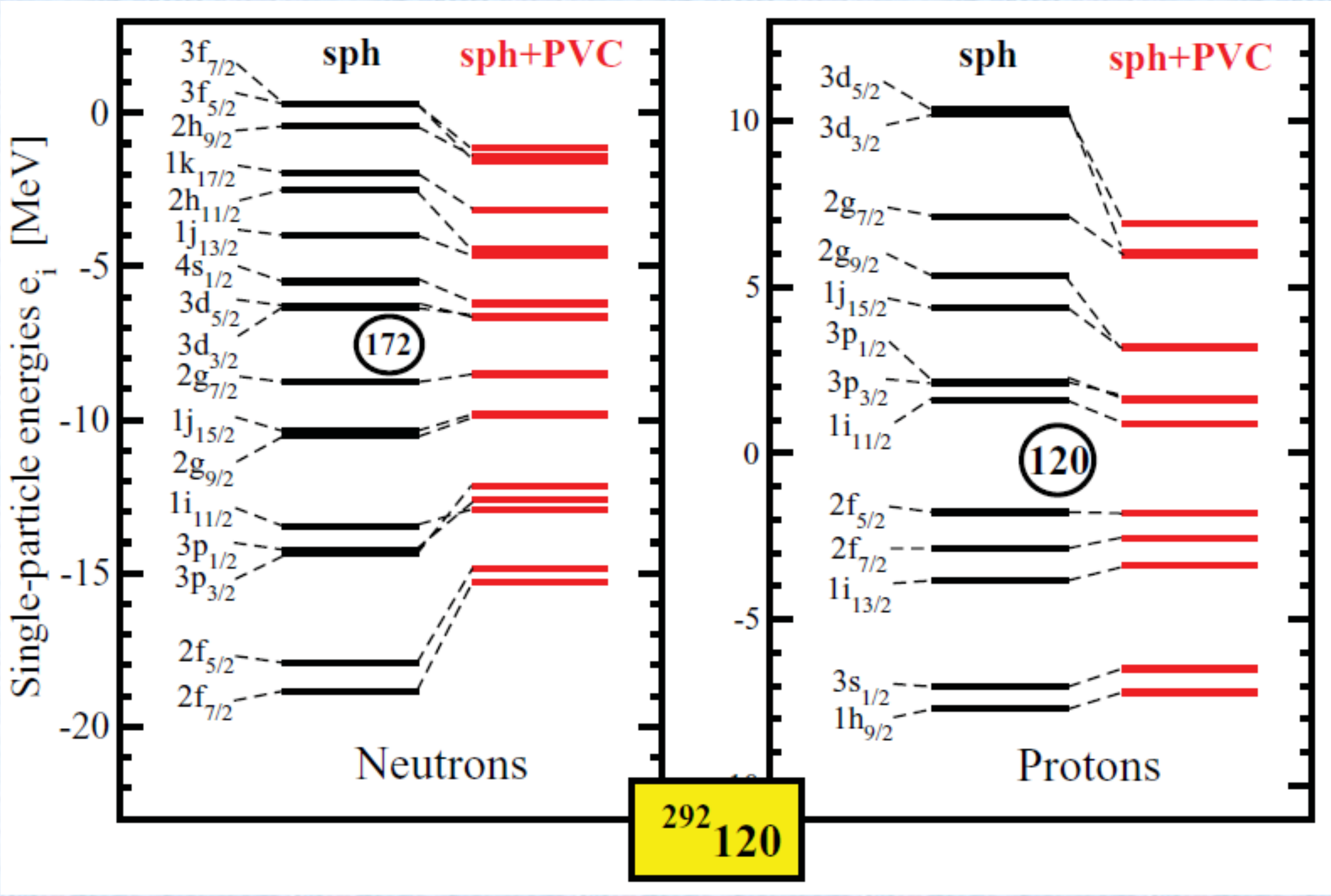

E. Litvinova, AA, PRC 84, 014305 (2011)

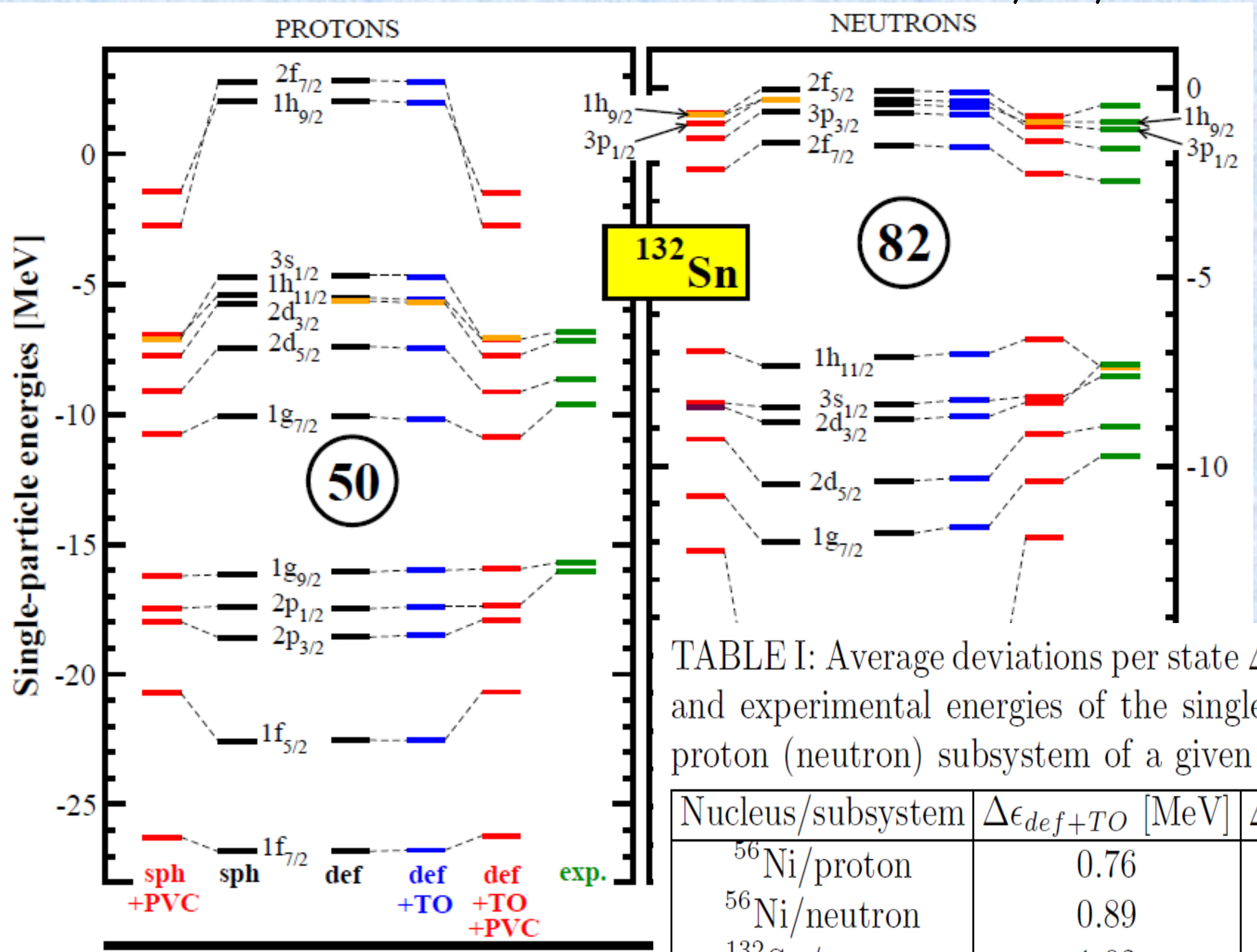

TABLE I: Average deviations per state $\Delta\epsilon$ between calculated and experimental energies of the single-particle states for a proton (neutron) subsystem of a given nucleus. The results

Nucleus/subsystem	$\Delta\epsilon_{def+TO}$ [MeV]	$\Delta\epsilon_{def+TO+PVC}$ [MeV]
^{56}Ni/proton	0.76	0.77
^{56}Ni/neutron	0.89	0.71
^{132}Sn/proton	1.02	0.68
^{132}Sn/neutron	0.89	0.39
^{208}Pb/proton	1.53	0.84
^{208}Pb/neutron	1.00	0.47

particle-vibration coupling
+ TO, TE polarization effects

Accuracy of the description of the ground states in odd-mass deformed nuclei in different approaches

Region (parametrization)	calculated states (#)	compared states (#)	correct ground states (%)
Actinides (NL3*)	415	209	38 %
Actinides (NL1)	444	217	45 %
Rare-earth (NL1)	360	149	48 %

CDFT
AA and S.Shawaqfeh, PLB 706 (2011) 177

Systematic Hartree–Fock+BCS calculations of deformed nuclei with SIII, SkM* and SLy5 Skyrme forces and FRDM calculations employing phenomenological folded-Yukawa potential[L. Bonneau et al, PRC 76 (2007) 024320]

Model	Sph.	Def.	Total
SIII	83.9% (90.8%) 183(+15)/218	40.5% (61.5%) 60(+31)/148	66.4% (79.0%) 242(+46)/365
SkM*	76.2% (89.2%) 218(+37)/286	37.5% (61.8%) 54(+35)/144	63.3% (80.0%) 272(+72)/430
SLy4	77.8% (85.8%) 186(+19)/239	39.3% (60.7%) 57(+32)/140	64.1% (77.6%) 243(+51)/379
FRDM	90.9% 90/99	43.1% 137/318	54.4% 227/417

3. Evolution of shapes and fission barriers as a function of Z and A.

The evolution of shapes of the ground states of SHE

Woods-Saxon potential,
M. Kowal, P. Jachimowicz, J. Skalski,
At.Data Nucl. Data Tables, subm.

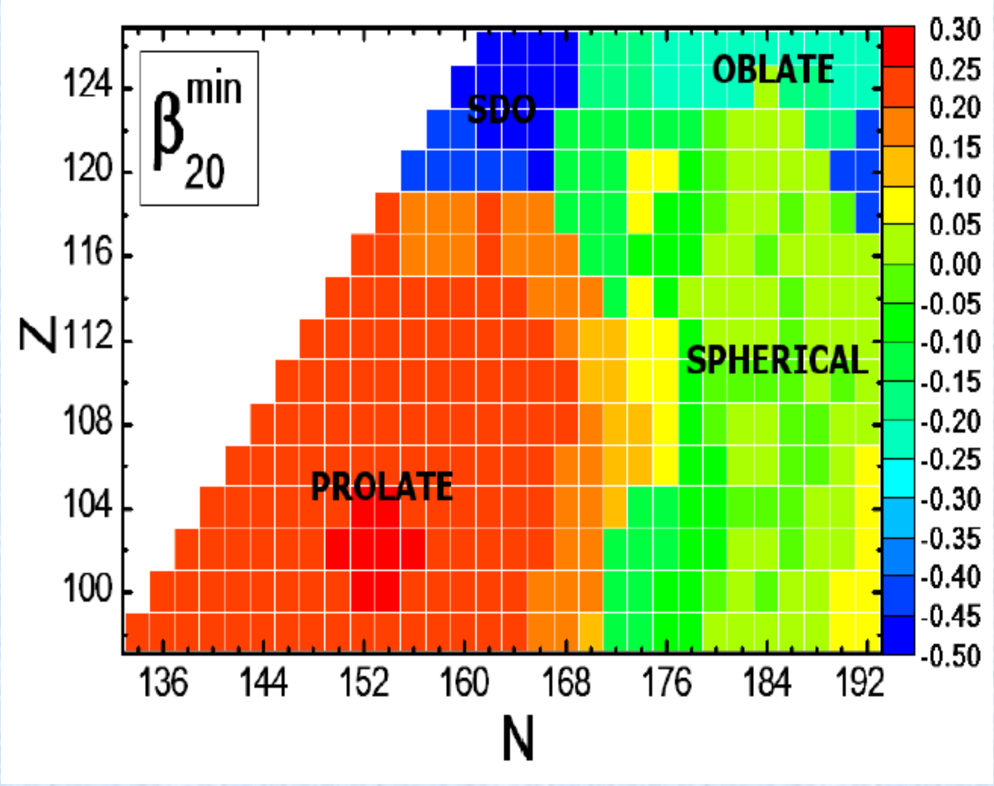

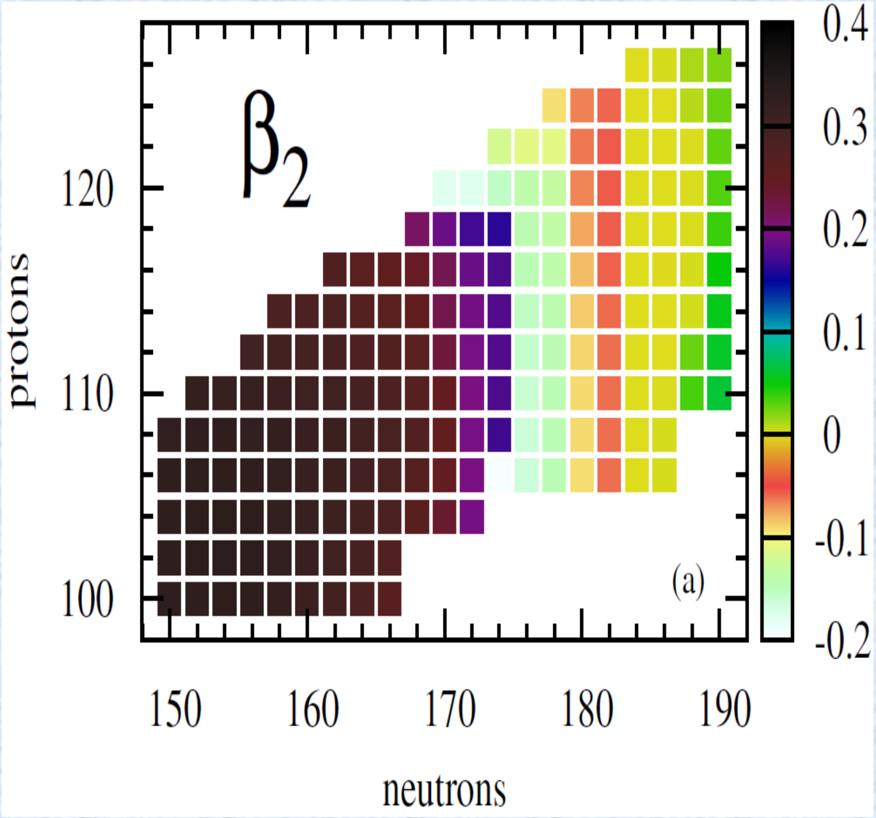

Gogny D1S
M. Warda, J.L. Egido,
PRC, in press

RMF(NL3*)+BCS

1. N_F=20 and N_B=20
2. $E_{cut\text{-}off}$ =120 MeV, monopole pairing
3. Q_{20} , Q_{22} constraints

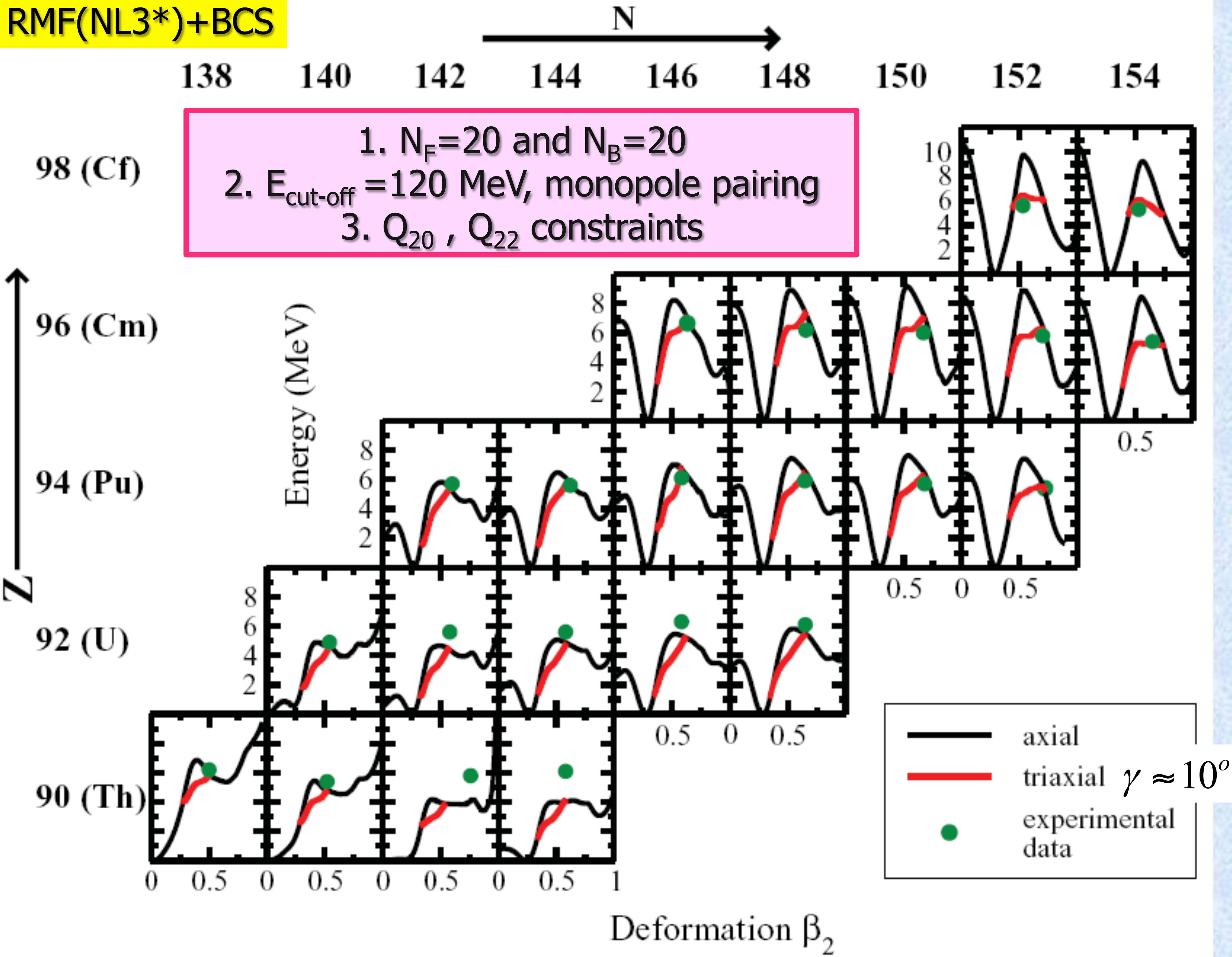

Fission barriers: theory versus experiment [state-of-the-art]

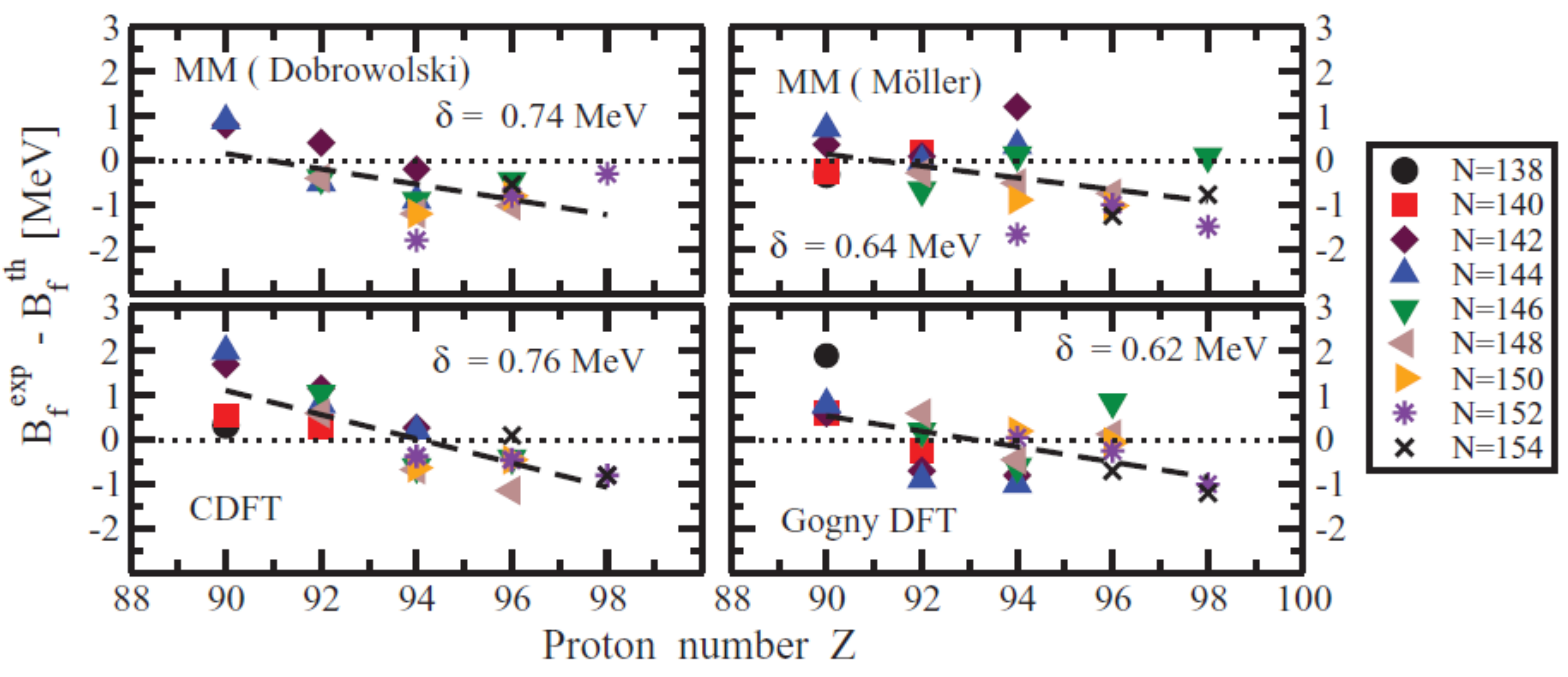

Mac+mic, LSD model
A.Dobrowolski et al,
PRC 75, 024613 (2007)

Mac+mic, FRDM model
P. Moller et al,
PRC 79, 064304 (2009)

Gogny DFT,
J.-P. Delaroche et al,
NPA 771, 103 (2006).

CDFT : actinides H. Abusara, AA and P. Ring, PRC 82, 044303 (2010)
superheavies: H. Abusara, AA and P. Ring, PRC 85, 024314 (2012)

UNEDF1 functional: focus on heavy nuclei and fission

Comparison with RIPL-3 (IAEA) data:

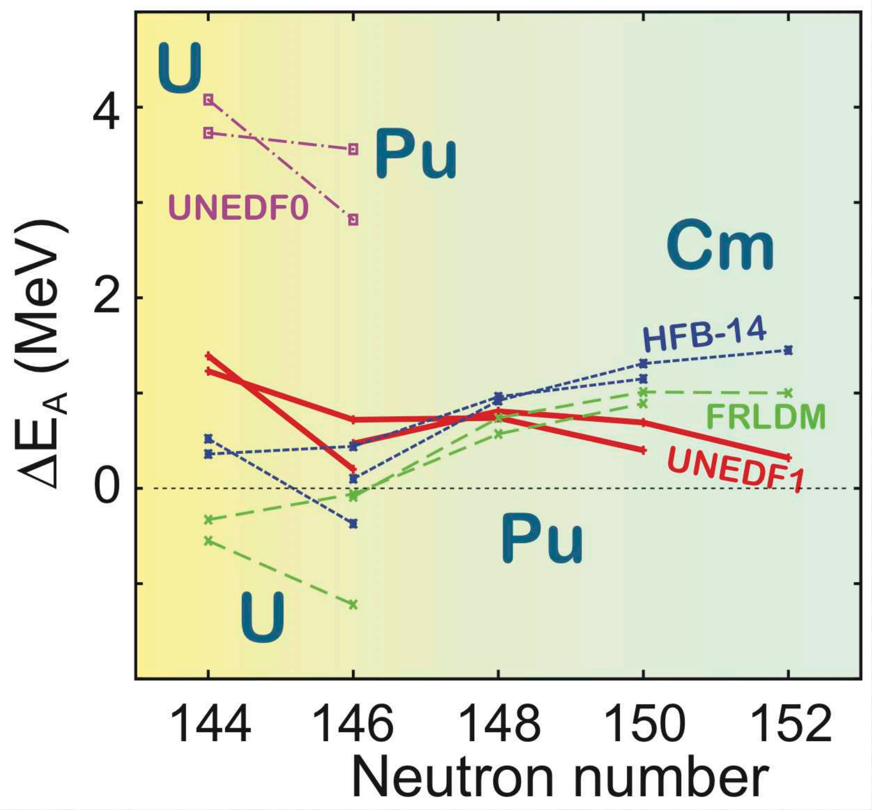

Fission barriers: theory versus experiment [state-of-the-art]

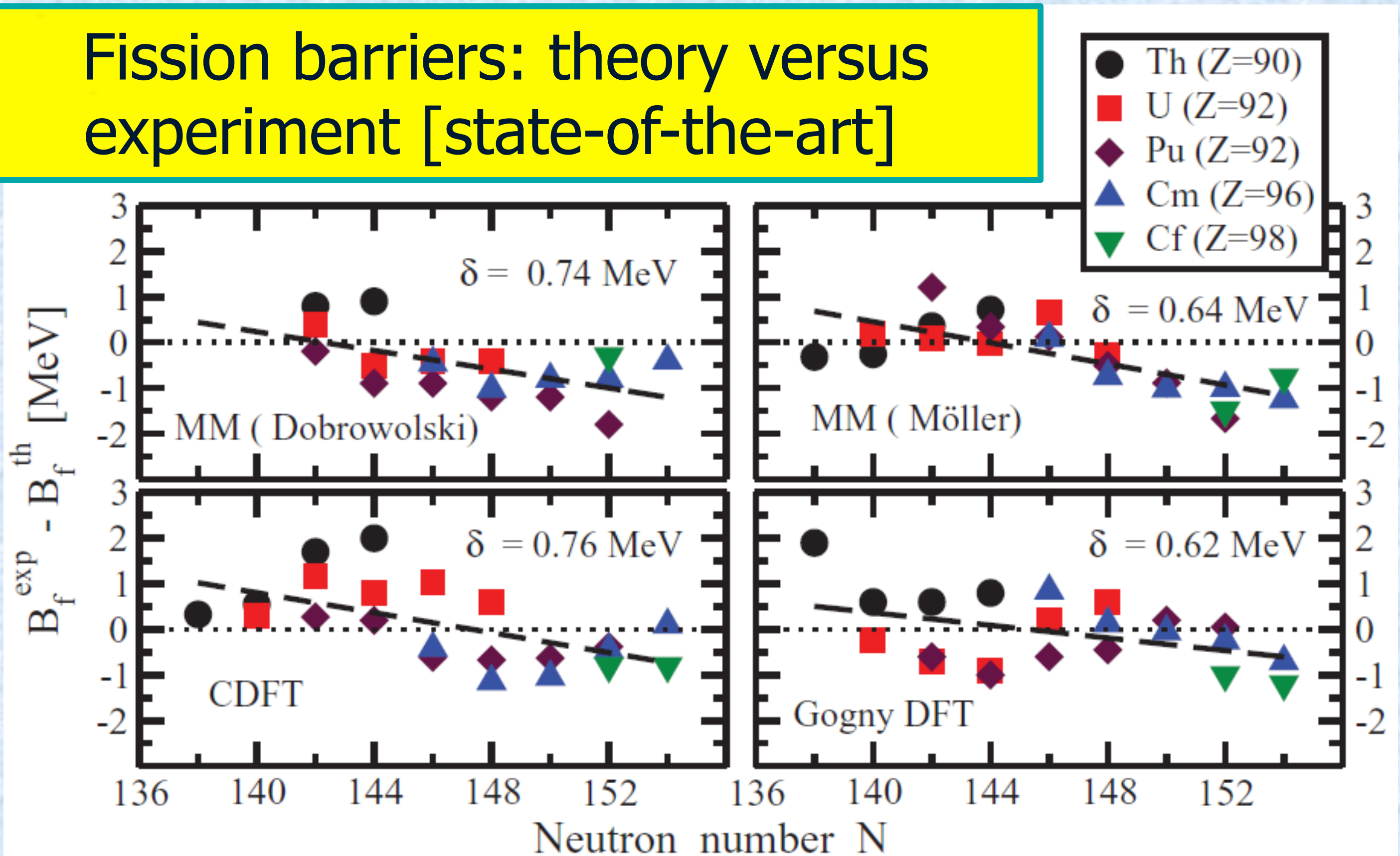

1. The accuracy of the description of inner fission barrier heights is not very sensitive to the accuracy of the description of single-particle energies and the effective mass of nucleon.

2. Among the DFT models which provide a reasonable description of the fission barrier heights, CDFT is the only one which does not fit the parameters to the inner fission barriers of actinides or their fission isomers.

Fission barriers: how accurate are experimental evaluations?

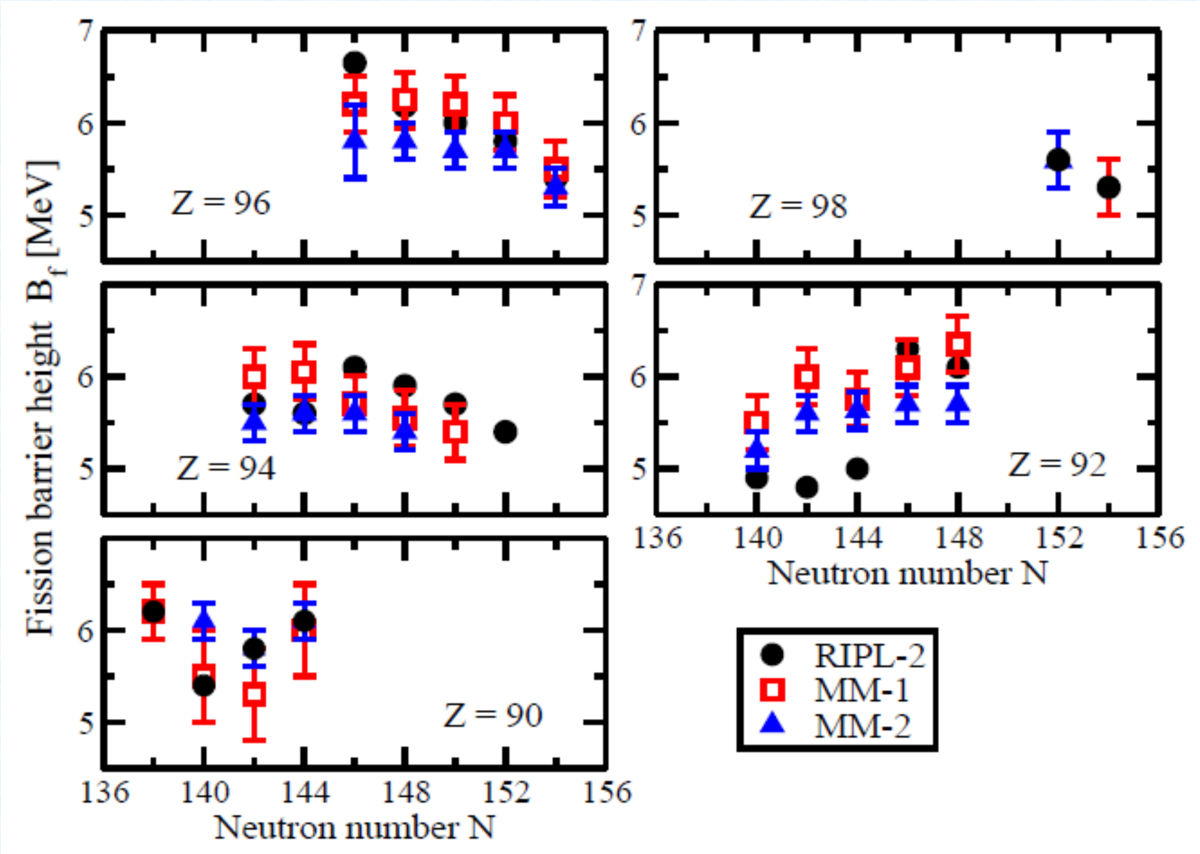

MM-1, MM-2

19. D. G. Madland and P. Möller, *Los Alamos National Laboratory unclassified report*, LA-UR-11-11447 (2011).
20. B. B. Back, O. Hansen, H. C. Britt and J. D. Garrett, *Phys. Rev. C* **9** (1974) 1924.
21. H. C. Britt, in *Proc. Symposium on the Physics and Chemistry of Fission*, Jülich, Germany, May 14–18, 1979 (IAEA, Vienna, 1980), Vol. I, p. 3.
22. S. Bjornholm and J. E. Lynn, *Rev. Mod. Phys.* **52** (1980) 725 and references therein.

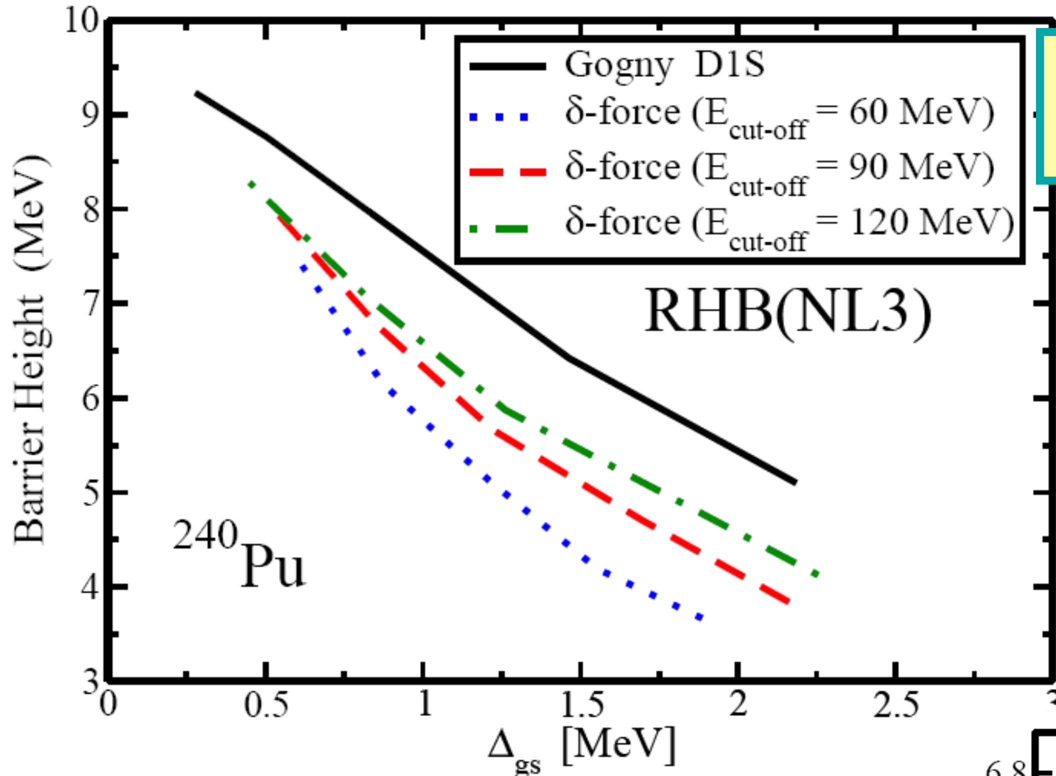

Dependence of the fission barrier height on the cut-off energy $E_{cut-off}$

Gogny force has finite range, which automatically guarantees a proper cut-off in momentum space

$$\Delta_{gs} = \frac{1}{2}(\langle\Delta\rangle_n + \langle\Delta\rangle_p)$$

defined in ND-minimum

$\delta - force$

$$\kappa_{12} = \sum_k \underbrace{V^*_{2k} U_{1k}}$$

includes high momenta and leads to a ultra-violet divergence

$E_{cut-off}$ **to avoid divergencies**

S.Karatzikos et al, PLB 689, 72 (2010)

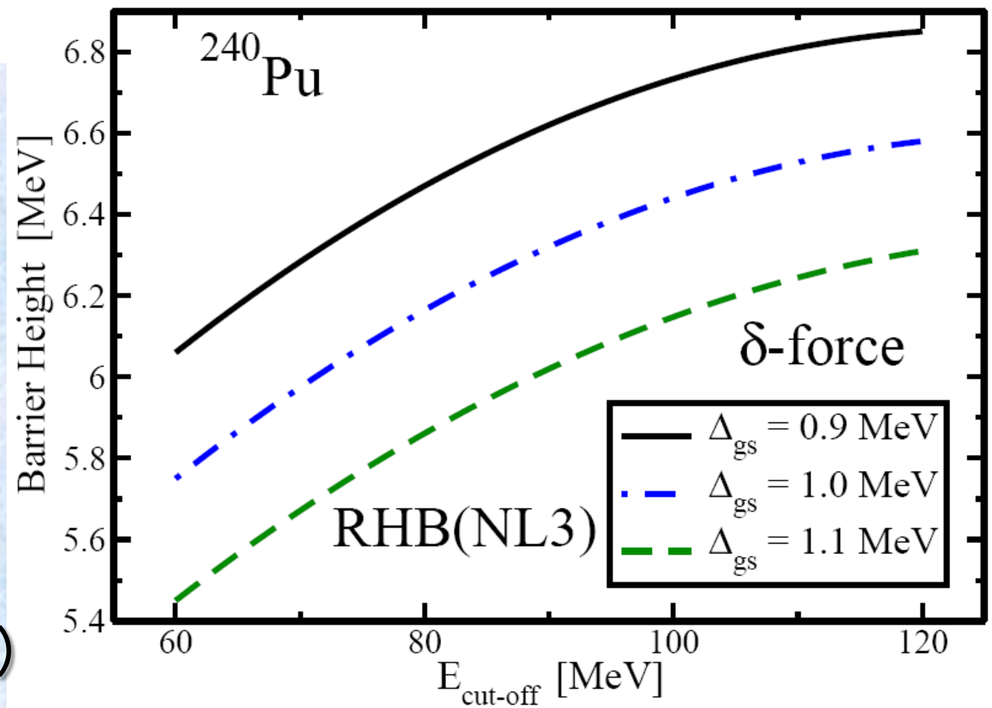

Triaxiality of fission barriers: the origin

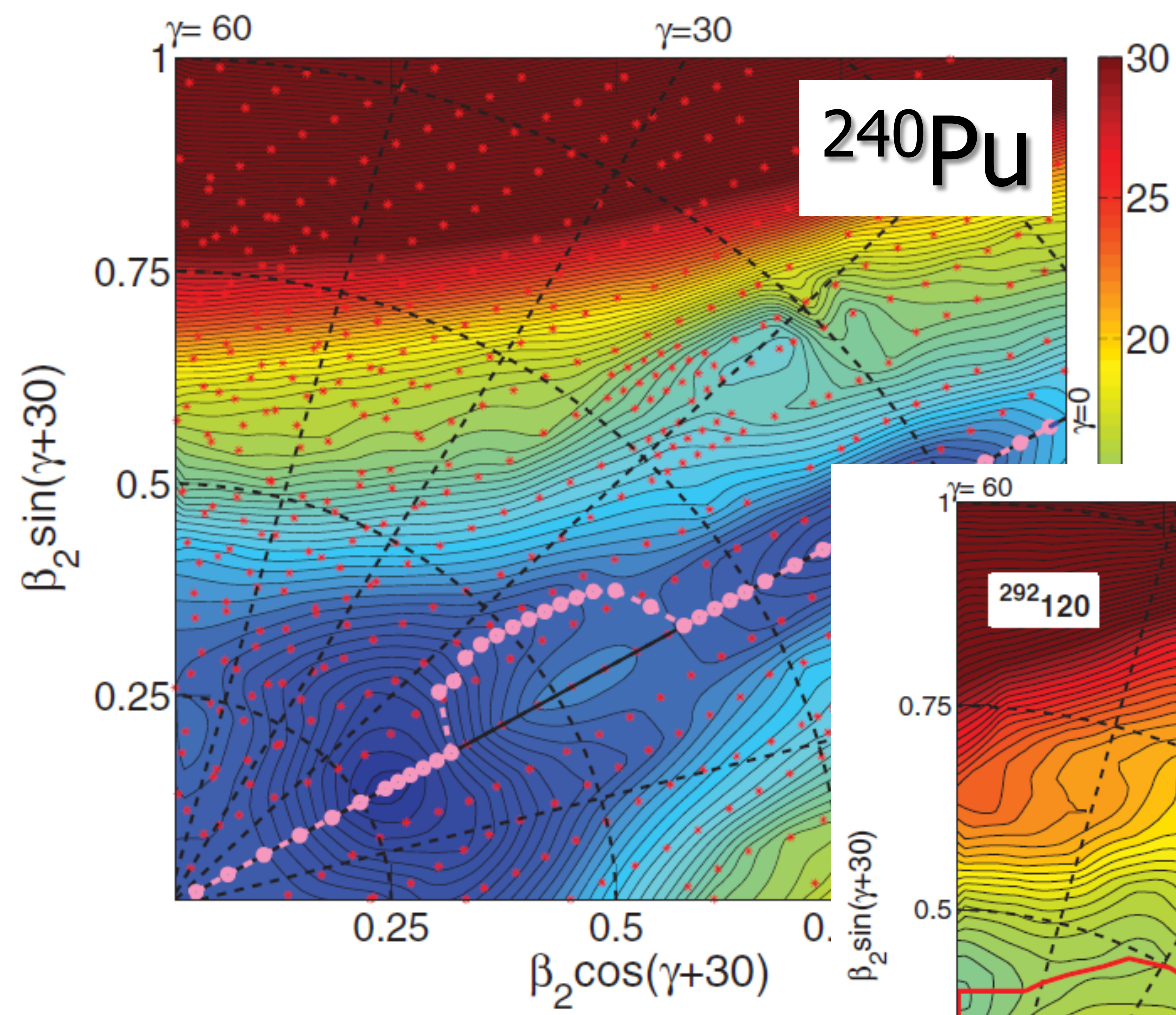

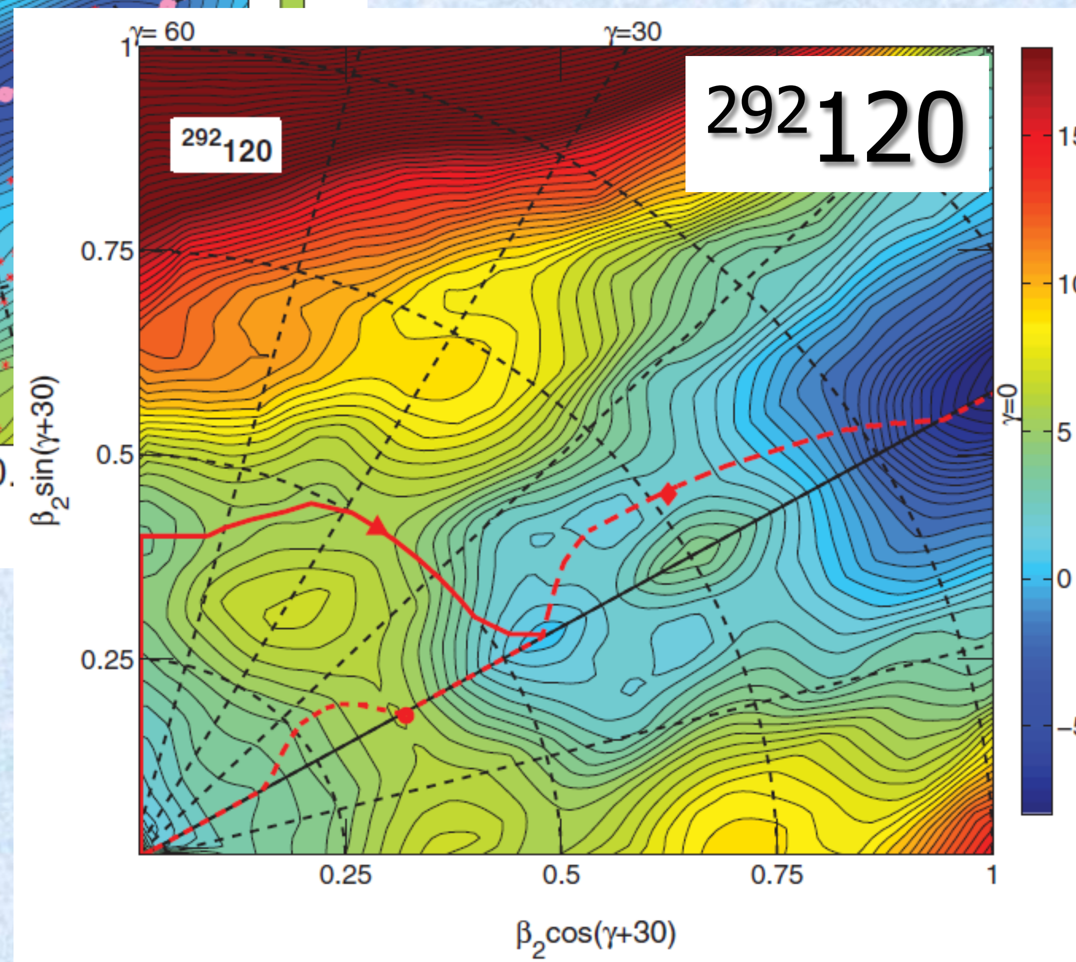

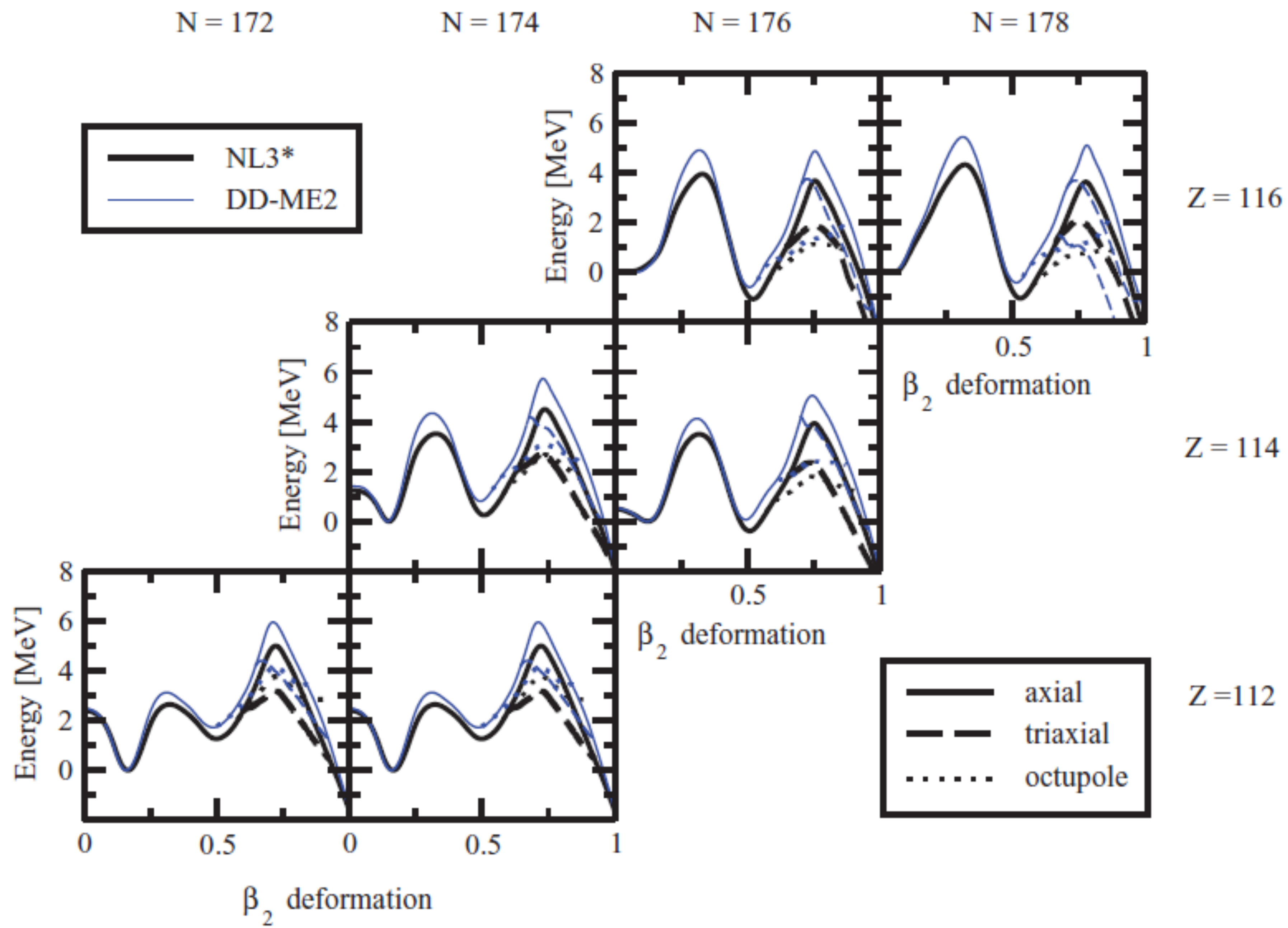
N = 172
N = 174
N = 176
N = 178
NL3*
DD-ME2
Z = 116
Z = 114
Z =112
axial
triaxial
octupole
Energy [MeV]
β2 deformation
0
0.5
1
0
2
4
6
8

Inner fission barrier height according to different models

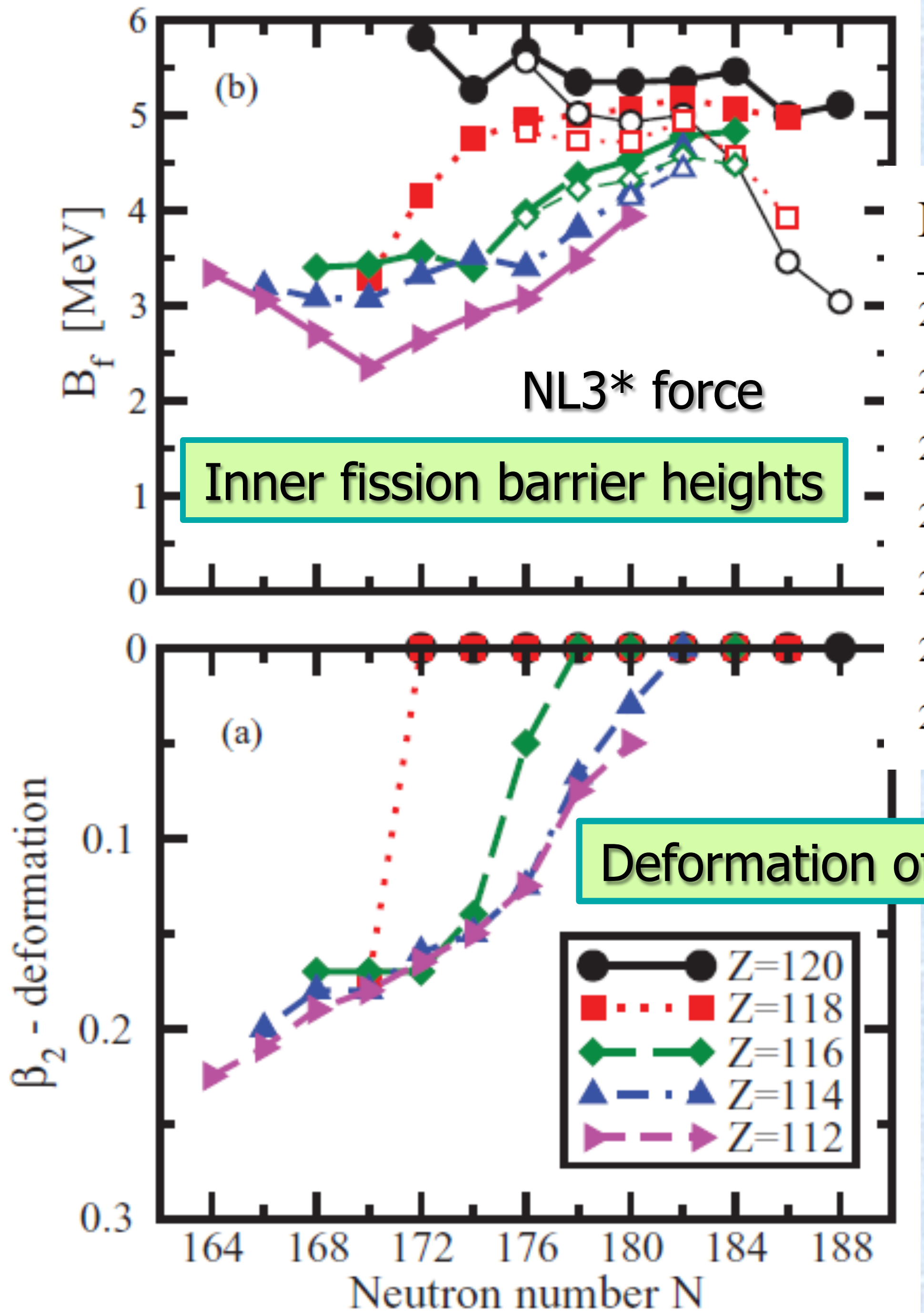

Nucleus	FRLDM	ETFSI	HN
$^{284}112_{172}$	7.41	2.2	4.29
$^{286}112_{174}$	8.24	3.6	5.01
$^{288}114_{174}$	9.18	6.1	5.53
$^{290}114_{176}$	9.89	6.6	5.83
$^{292}114_{178}$	9.98	7.2	6.34
$^{292}116_{176}$	9.26	6.5	6.22
$^{294}116_{178}$	9.46	7.2	6.28

M. Kowal et al,
PRC 82, 014303 (2010)

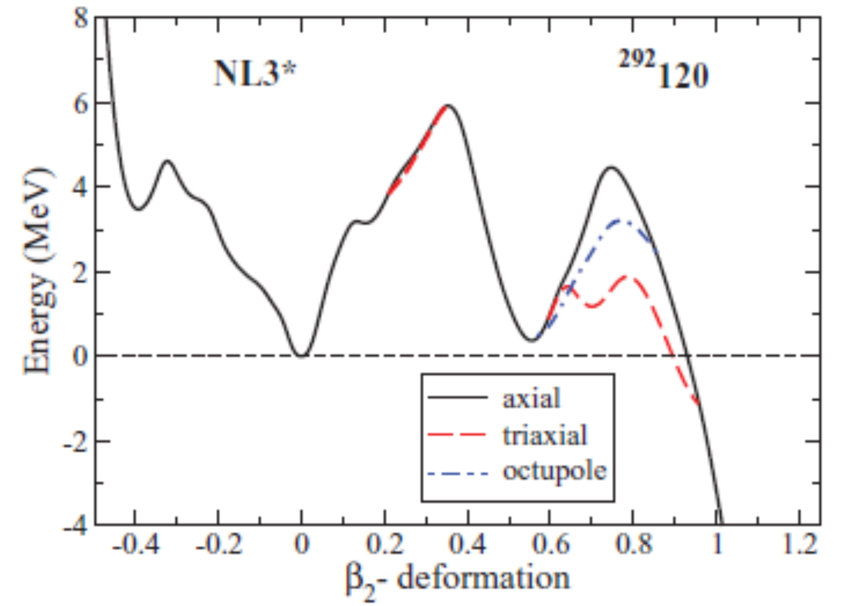

NL3*
$^{292}120$
Energy (MeV)
β_2- deformation
axial
triaxial
octupole

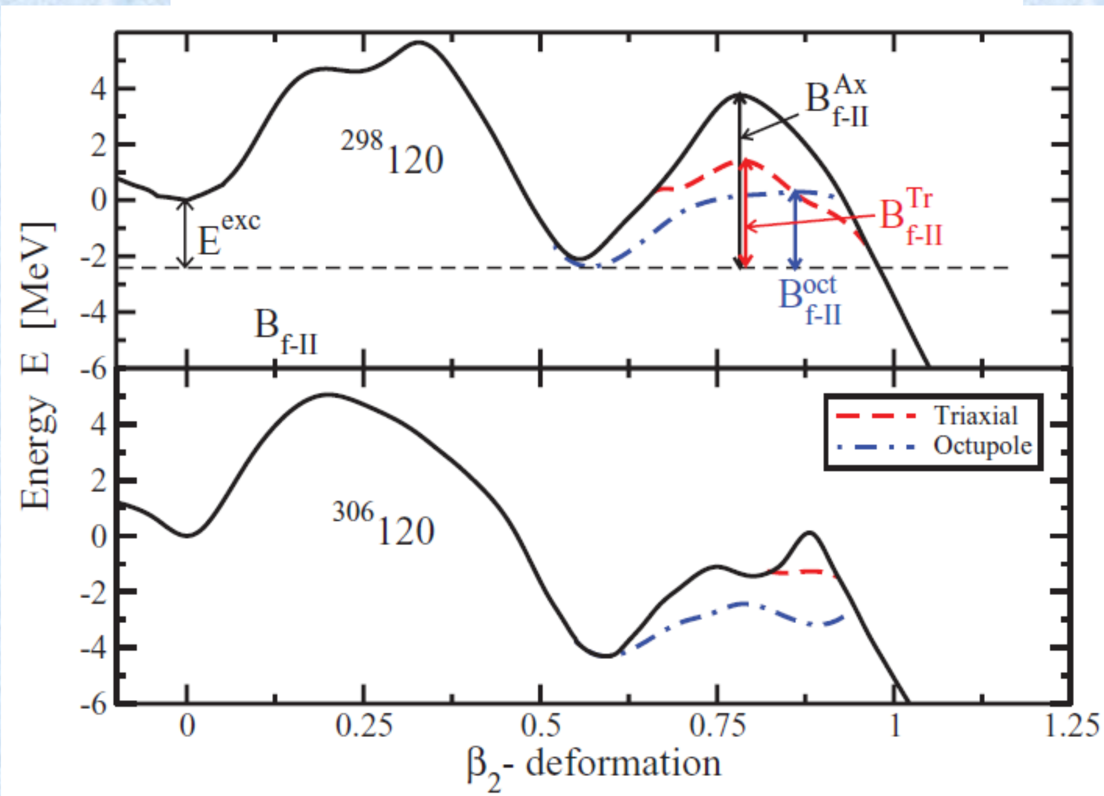

$^{298}120$
$B^{Ax}_{f\text{-}II}$
$B^{Tr}_{f\text{-}II}$
$B^{oct}_{f\text{-}II}$
E^{exc}
$B_{f\text{-}II}$
$^{306}120$
Triaxial
Octupole
Energy E [MeV]
β_2- deformation

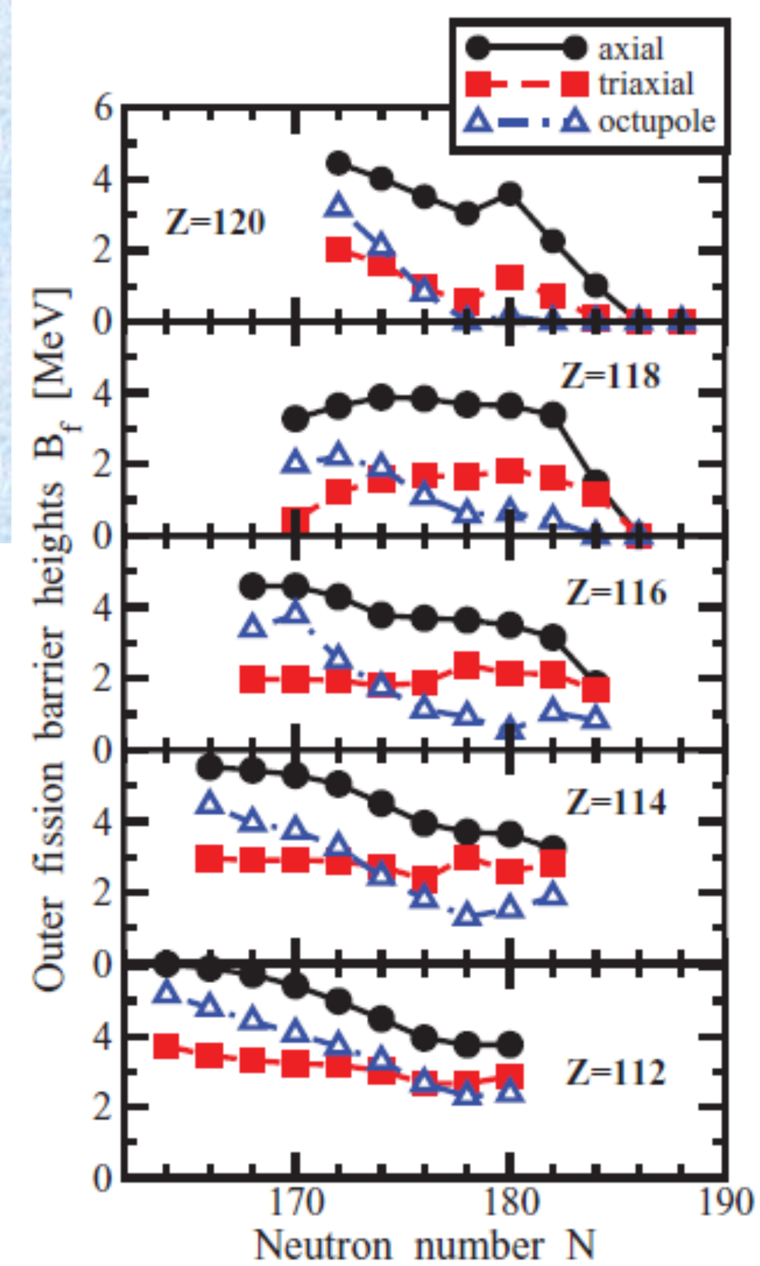

axial
triaxial
octupole
Z=120
Z=118
Z=116
Z=114
Z=112
Outer fission barrier heights B_f [MeV]
Neutron number N

Conclusions:

1. At present stage, neither of the possibilities for gap combinations:

   $Z=114$, $N=184$ (mic+mac)

   $Z=120$, $N=172$ (CDFT)

   $Z=126$, $N=184$ (Skyrme)

   can be ruled out based on available experimental data or theoretical arguments.

2. The accuracy of the description of fission barriers in DFT approaches has reached the one of mic+mac approaches. However, this does not mean that the predictions for fission barriers in superheavy nuclei converge: the differences between the different classes of the models or even within one class of models [dependence on the parametrization] still exists.

In the rush of creation,
the God forgot to write down
the effective interaction he used.

S˜ao Paulo potential as a tool for calculating *S factors of fusion reactions in dense stellar matter*

L. R. Gasques, AA et al, PRC 76, 045802 (2007).

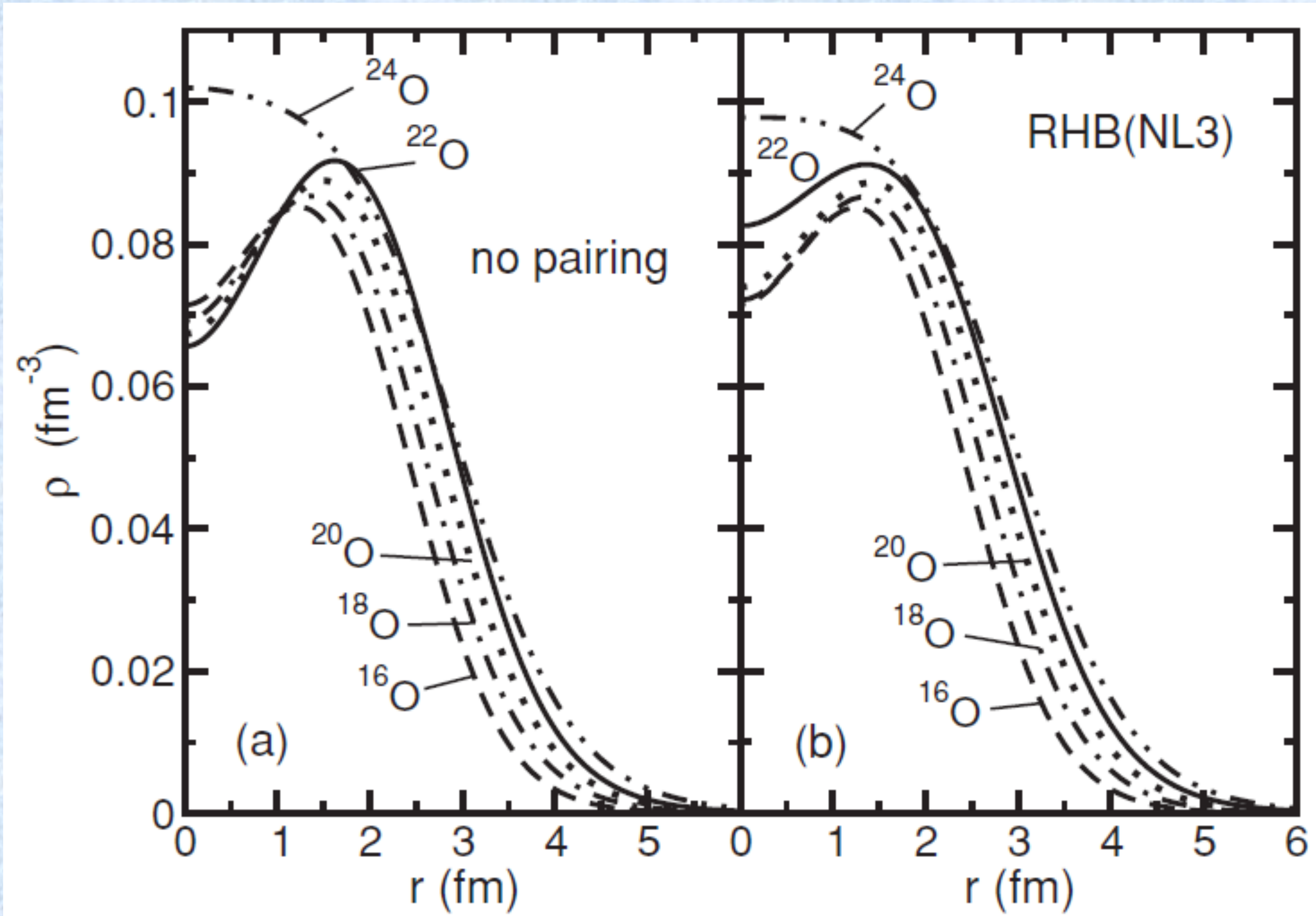

AA and S.Frauendorf, PRC 71, 024308 (2005)

'g-s' – ground state configuration

'exc-s' – excited state configuration

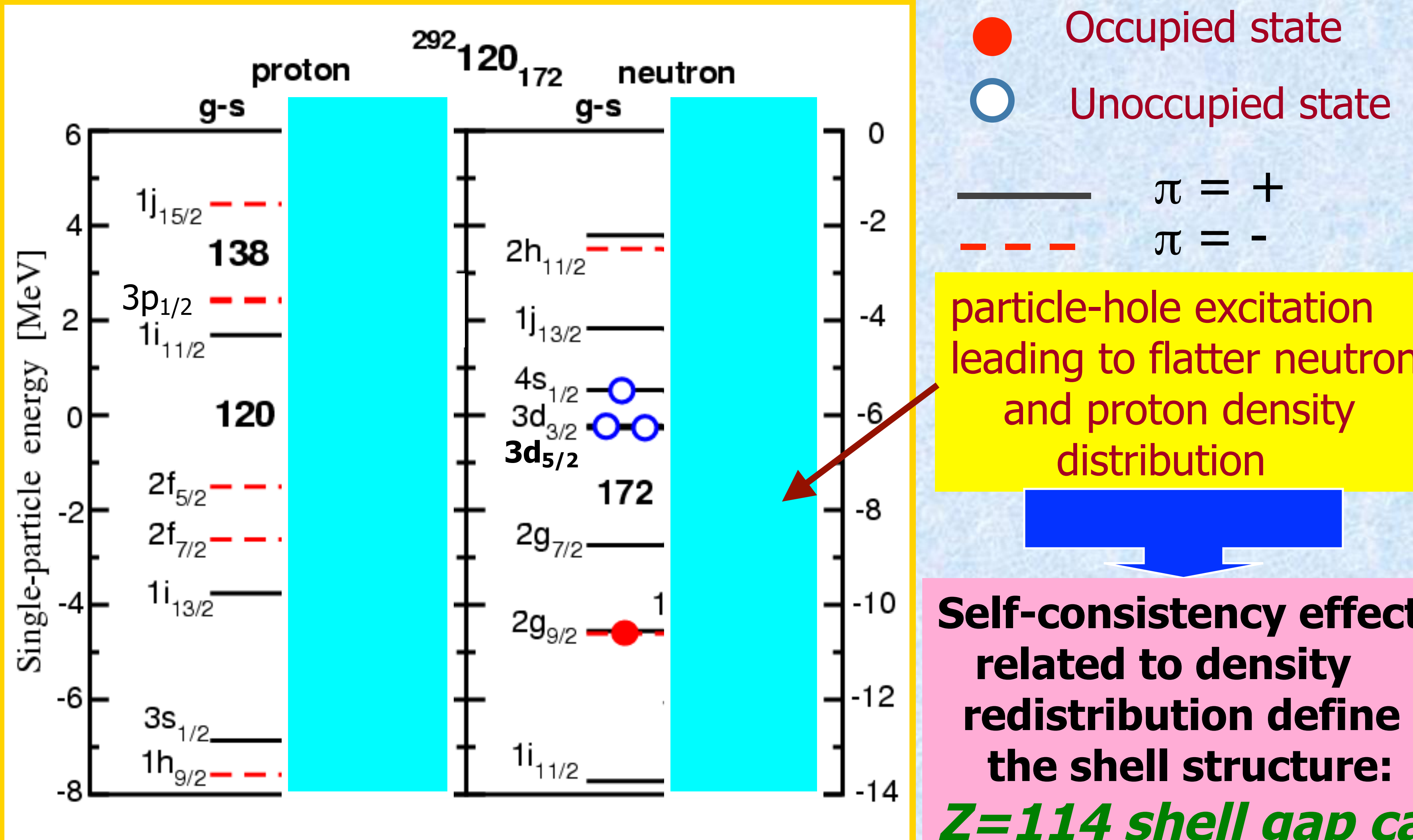

particle-hole excitation leading to flatter neutron and proton density distribution

Self-consistency effects related to density redistribution define the shell structure:

Z=114 shell gap can be excluded

Spherical RMF calculations with NL3 forces

Accuracy of the description of the energies of deformed one-quasiparticle states in actinides in RHB calculations: **correction for low Lorentz effective mass**

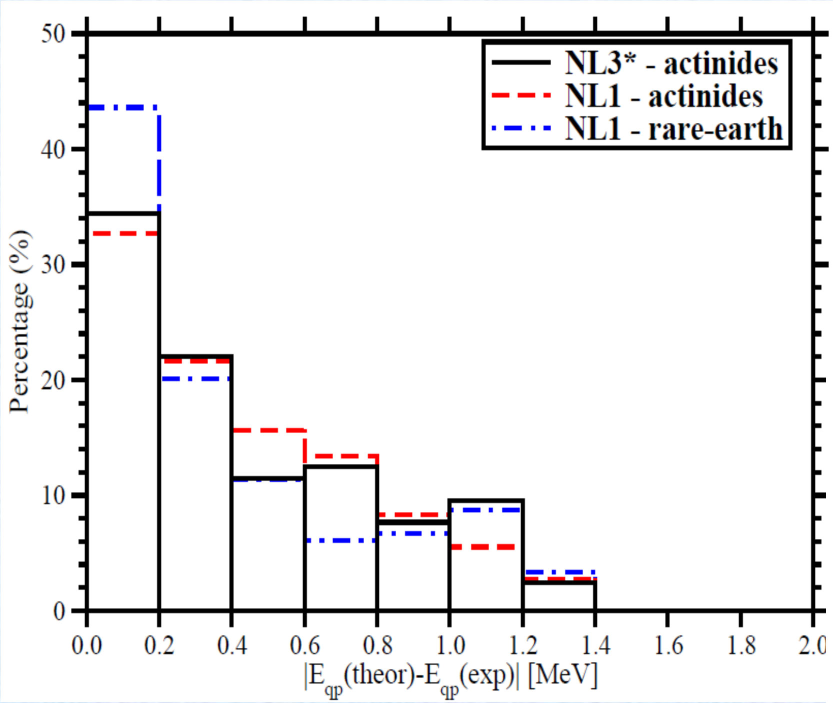

Energy scale is corrected for low effective mass

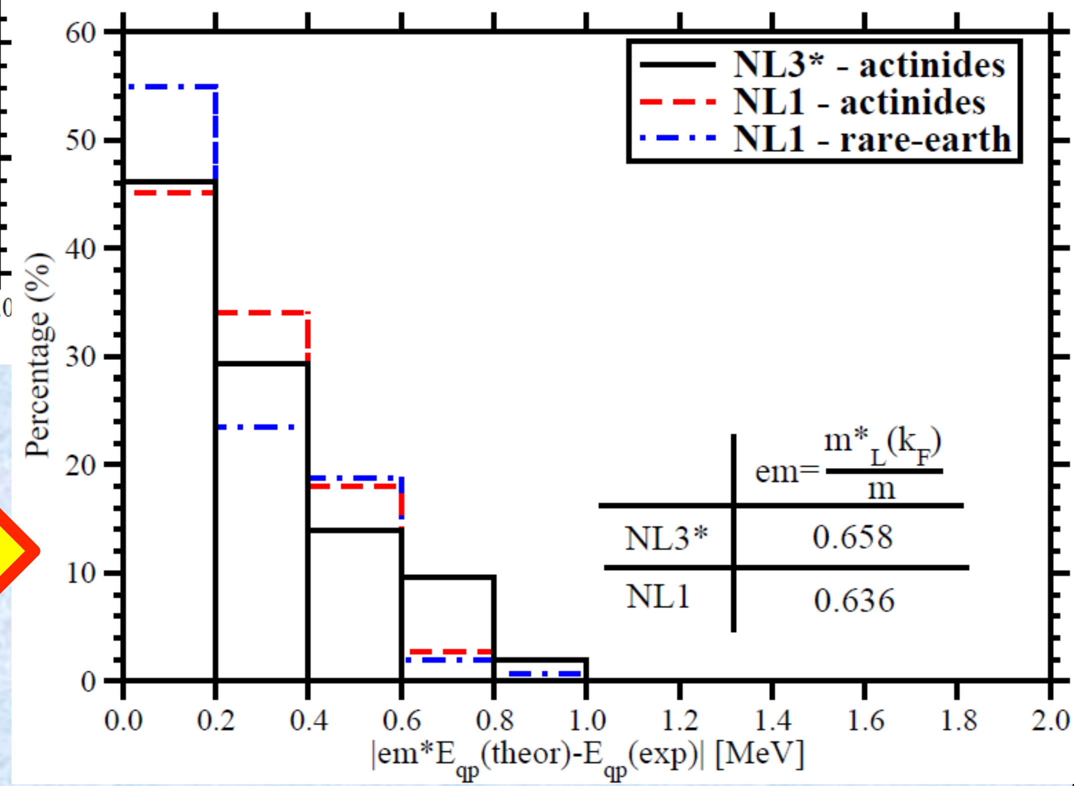

1. 75-80% of the states are described with an accuracy of phenomenological (Nilsson, Woods-Saxon) models
2. The remaining differences are due to incorrect relative energies of the single-particle states

Triaxiality and gamma-softness of the ground states of SHE

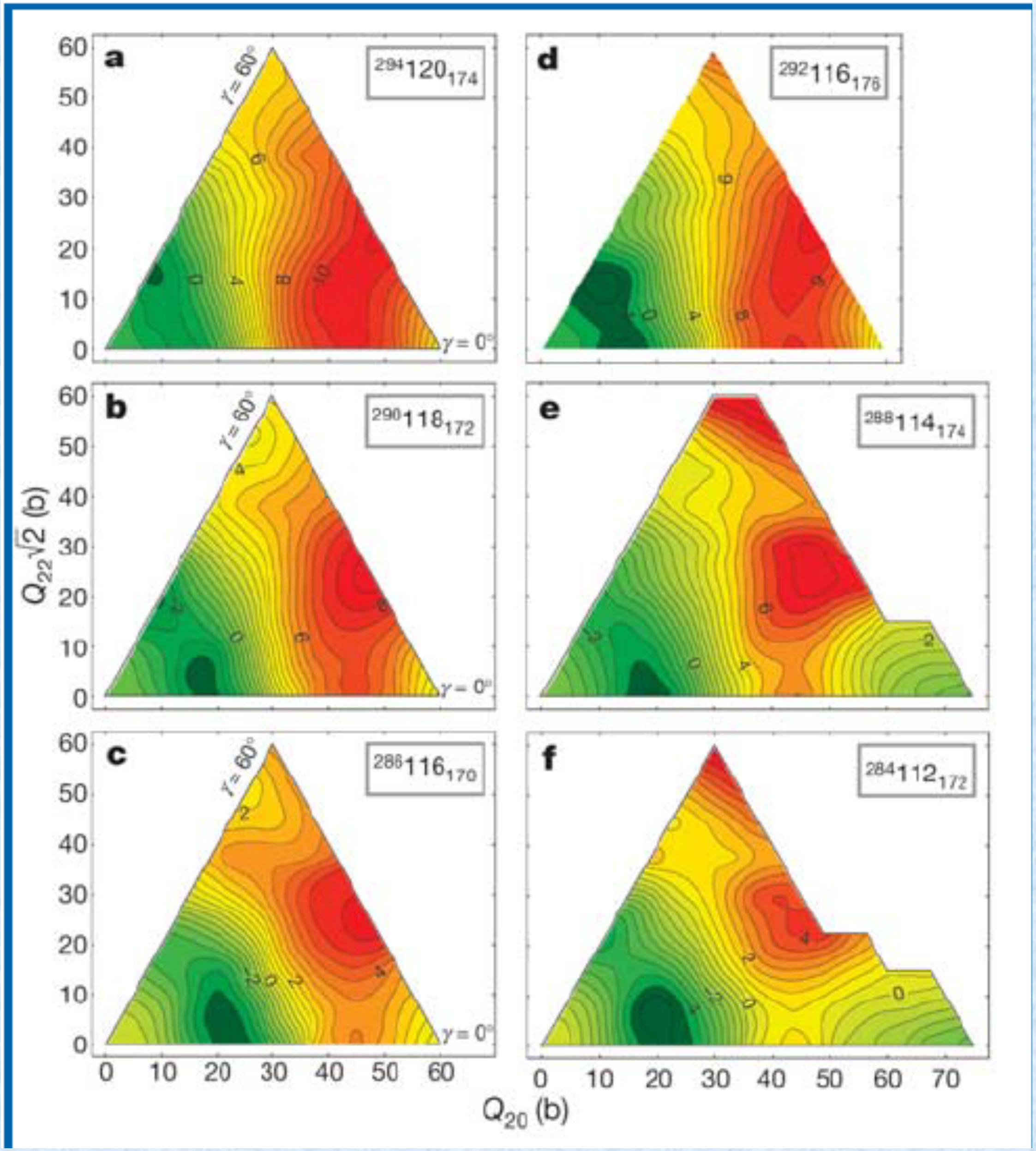

S. Cwiok, P.-H. Heenen, W. Nazarewicz, Nature 433, 705 (2005)

Dependence of neutron N=172 and 184 gaps on CDFT parametrization and neutron number

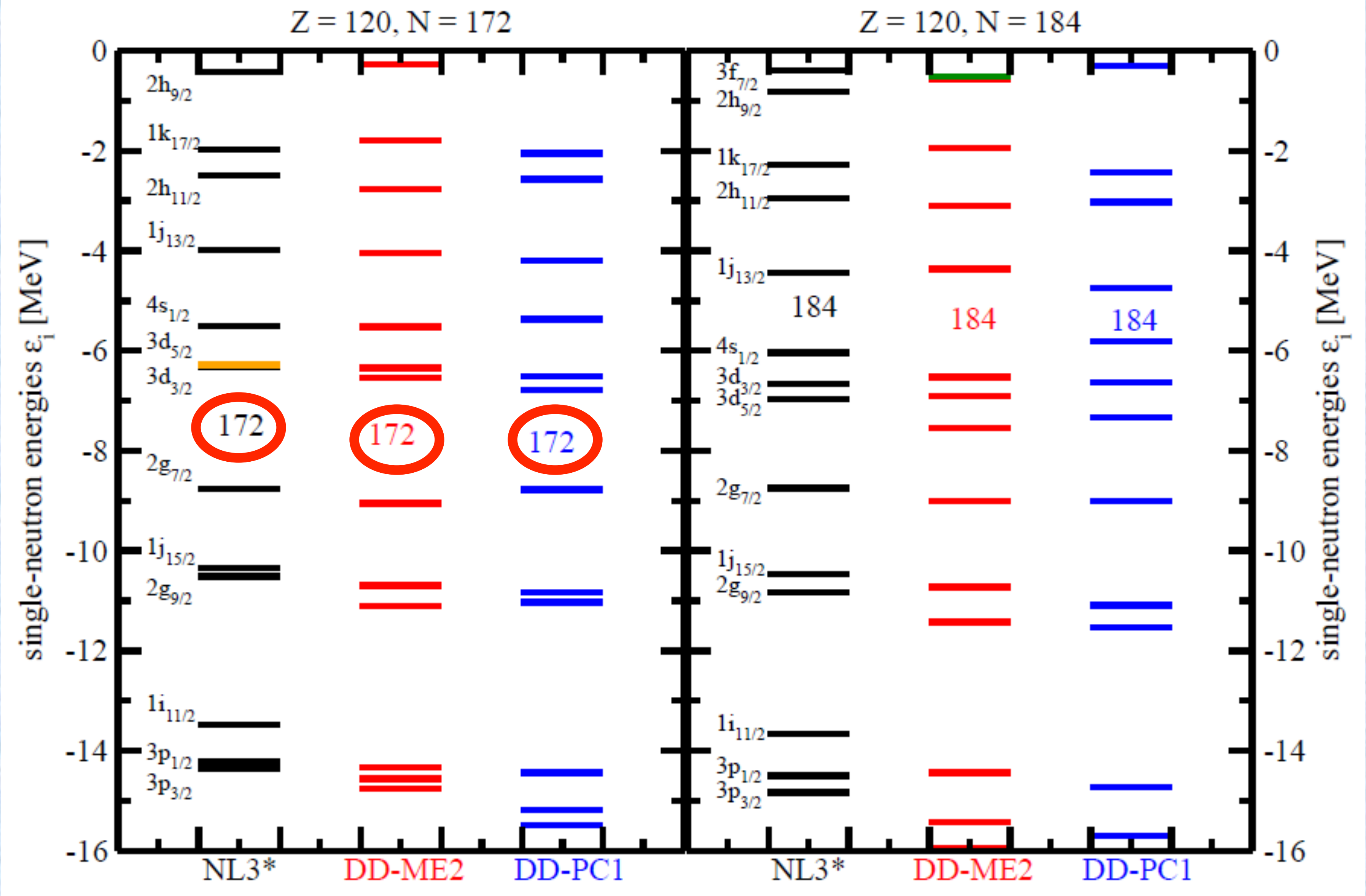

Dependence of proton Z=120 gap on CDFT parametrization and neutron number

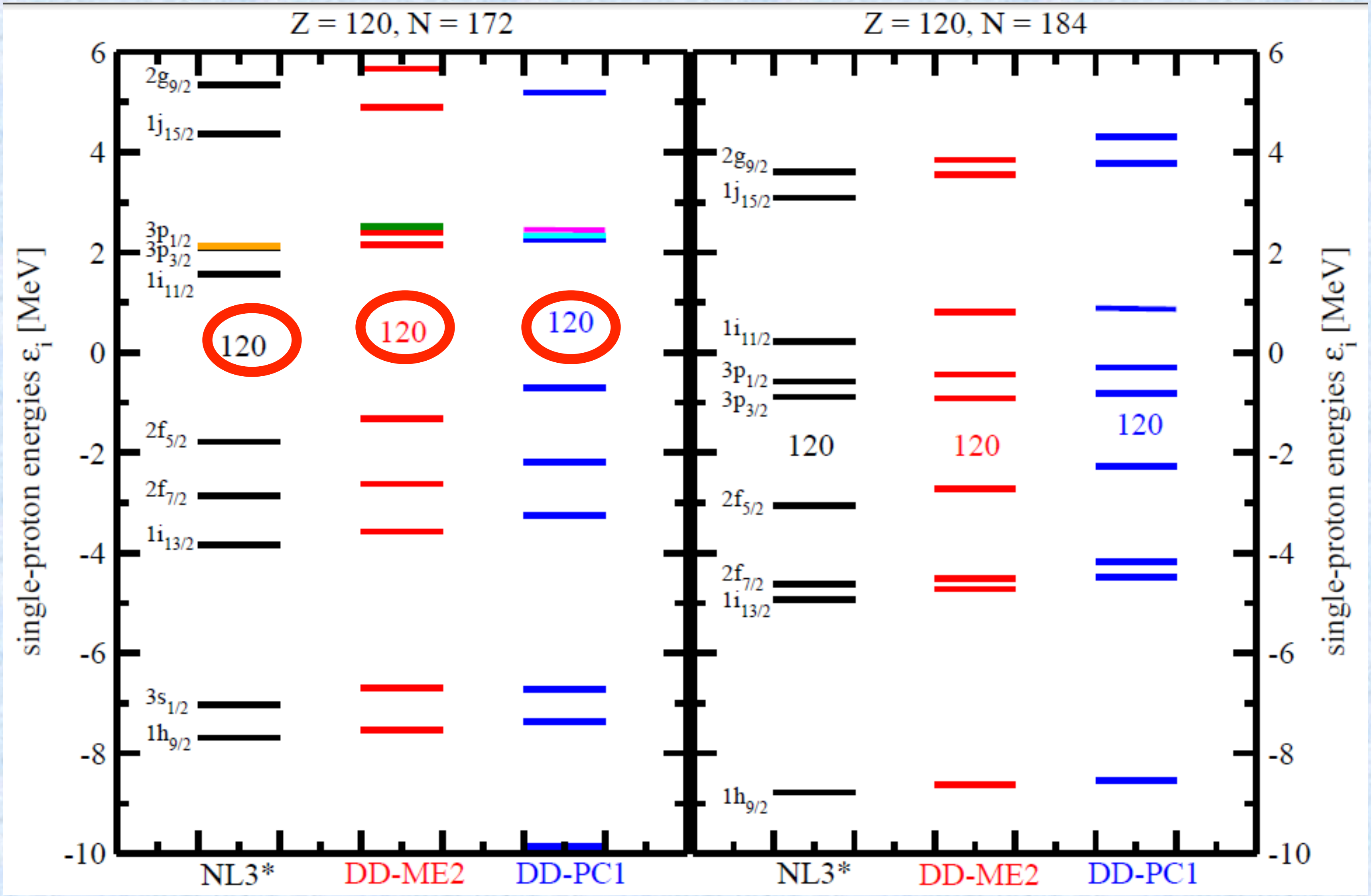

Lesson from quantum mechanics: spherical harmonic oscillator

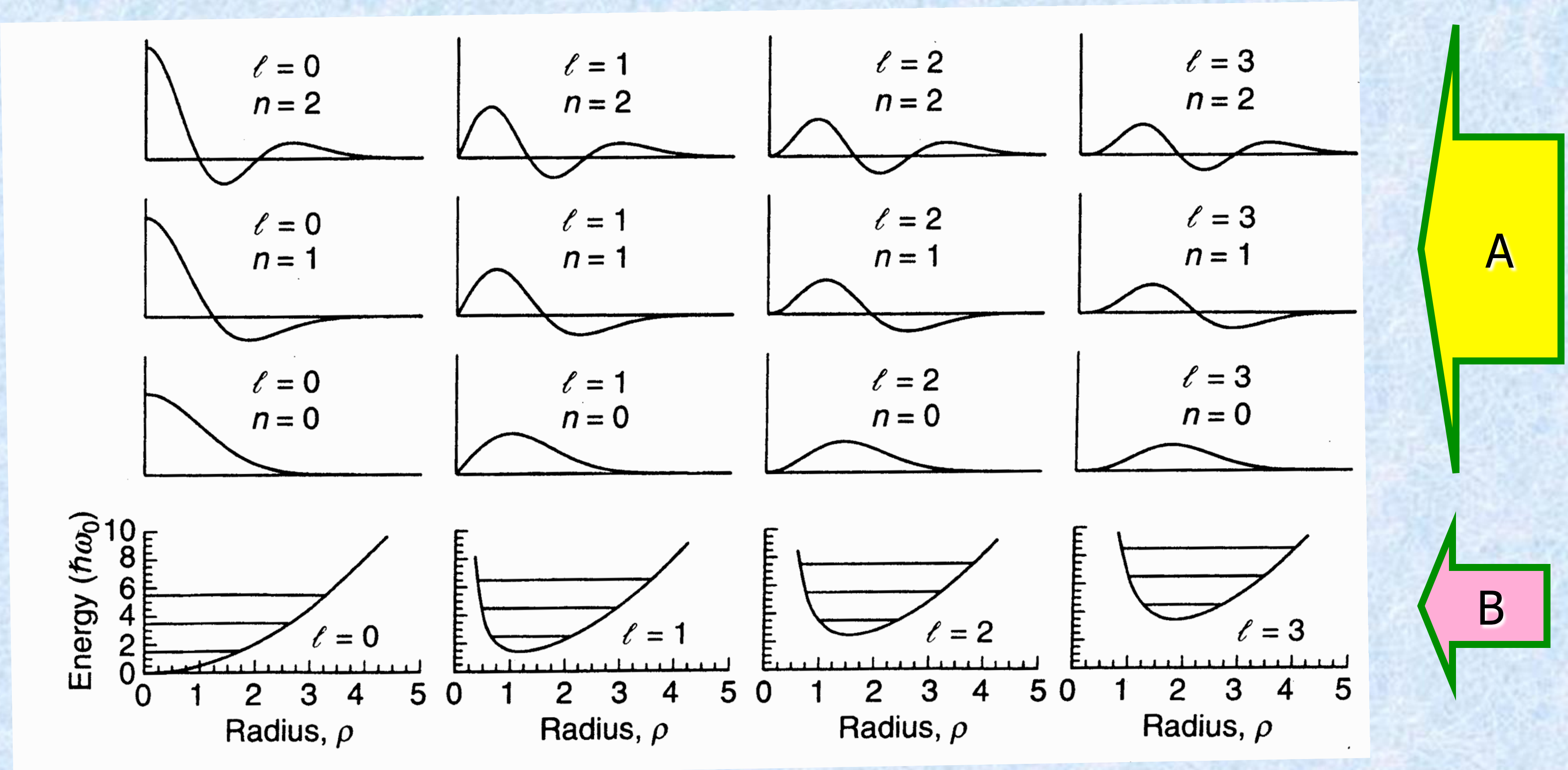

A: the radial wave function $R(\rho)$

B: effective radial potential, i.e. with the centrifugal term

$$\hbar^2 \ell(\ell+1)/(2Mr^2)$$ added.

CDFT analysis of single-particle energies in spherical Z=120, N=172 nucleus

corrected by the empirical shifts obtained in the detailed study of quasiparticle spectra in odd-mass nuclei of the deformed A~250 mass region (PRC 67 (2003) 024309)

Self-consistent solution